



**Kaunas University of Technology**

Faculty of Chemical Technology

# **Design, Synthesis and Investigation of Coumarine Based Compounds**

Master's Final Degree Project

---

**Nizy Sara Samuel**

Project author

**Dr. Dalius Gudeika**

Supervisor

---

**Kaunas, 2020**



**Kaunas University of Technology**

Faculty of Chemical Technology

# **Design, Synthesis and Investigation of Coumarine Based Compounds**

Master's Final Degree Project  
Chemical Engineering (6211EX020)

---

**Nizy Sara Samuel**

Project author

**Dr. Dalius Gudeika**

Supervisor

**Lect. Gintarė Kručaitė**

Reviewer

---

**Kaunas, 2020**



**Kaunas University of Technology**

Faculty of Chemical Technology

Nizy Sara Samuel

## **Design, Synthesis and Investigation of Coumarine Based Compounds**

### Declaration of Academic Integrity

I confirm that the final project of mine, Nizy Sara Samuel, on the topic „Design, Synthesis and Investigation of Coumarine Based Compounds“ is written completely by myself; all the provided data and research results are correct and have been obtained honestly. None of the parts of this thesis have been plagiarised from any printed, Internet-based or otherwise recorded sources. All direct and indirect quotations from external resources are indicated in the list of references. No monetary funds (unless required by Law) have been paid to anyone for any contribution to this project.

I fully and completely understand that any discovery of any manifestations/case/facts of dishonesty inevitably results in me incurring a penalty according to the procedure(s) effective at Kaunas University of Technology.

---

(name and surname filled in by hand)

---

(signature)



**Kaunas University of Technology**

Faculty of Chemical Technology

I confirm:

Dean of Faculty of Chemical Technology  
Prof. K. Baltakys

Coordinated with:

Head of the Department of Polymer  
Chemistry and Technology  
Doc. Joana Bendoraitienė

Decree of the Dean No.ST18-F-02-03  
2020 April 22

2020 April 22

**Task of the Master's final degree project**

Topic of the project (Design, Synthesis and Investigation of Coumarine Based Compounds)

Aim of the work and tasks

The aim of this work is synthesis and study of properties of coumarin based compounds for optoelectronic devices.

Tasks:

1. Synthesis and characterization of coumarin based compounds having trifluoromethyl fragments.
2. Study of the thermal, photophysical, electrochemical and photoelectrical properties of the obtained products.
3. Development of a technological scheme for the production of the synthesized compounds.

Requirements and conditions

There must be all mandatory parts in the final project as specified by „Methodological Requirements for the Preparation and Defense of Final Projects of the First-Degree Program Chemical Technology and Second-Degree Program Chemical Engineering“ approved by Dean Decree No. V25-02-02 (March 29 2019)

Supervisor

\_\_\_\_\_ (position, name, surname, signature)

\_\_\_\_\_ (date)

Task received: \_\_\_\_\_

(name, surname)

\_\_\_\_\_

(signature, date)

Samuel, Nizy Sara. Design, Synthesis and Investigation of Coumarine Based Compounds. Master's Final Degree Project supervisor:

Dr. Dalius Gudeika; Faculty of Chemical Technology, Kaunas University of Technology.

Study field and area: Engineering Sciences, Chemical Engineering

Keywords: coumarin, phenoxazine, fluorescence, optoelectronics, organic electroluminescent materials

Kaunas, 2020. 61 pages.

### **Summary**

The ever increasing need for organic luminescent materials in the field of optoelectronics have led to several research studies across the world. Organic functional materials possessing high stability and solubility are focussed for economical optoelectronic devices. Over the years, coumarins have found applications in optoelectronic devices owing to their myriad of characteristics especially their intrinsic optical properties and ease of synthesis. Here in this study, coumarin derivatives substituted with trifluoromethyl moiety at different positions was opted as the acceptor core and conjugated with strong donor — phenoxazine. Four coumarin based derivatives were designed and synthesized with relatively high reaction yields. Various characteristics such as photophysical, electrochemical and thermal of the synthesized compounds were investigated. Analysis of the effect of heat on the target compounds was done using differential scanning calorimetry and thermogravimetric analysis. It was found that the materials were thermally stable with glass forming abilities. Electrochemical properties were perceived by performing cyclic voltammetry and similar ionization potential values (5.09 eV), high enough for optoelectronic devices was obtained. Photophysical properties of the coumarin derivatives were observed by absorption and emission spectrometry. They revealed similar photophysical behaviour with fluorescence quantum yields of solid films in the range from 0.3 to 0.8. The materials synthesized showed solvatochromism, confirming intramolecular charge transfer in the structure. With an idea to extend the findings to practical application, a technological line was designed and proposed.

Samuel, Nizy Sara. Kumarino junginių projektavimas, sintezė ir tyrimas. Magistro baigiamasis projektas, vadovas dr. Dalius Gudeika : Kauno technologijos universitetas, Cheminės technologijos fakultetas.

Studijų kryptis ir sritis (studijų krypčių grupė): Inžinerijos mokslai, Chemijos inžinerija.

Reikšminiai žodžiai: kumarinas, fenoksazinas, fluorescencija, optoelektronika, organinės elektroliuminescencinės medžiagos,

Kaunas, 2020. 61 p.

### **Santrauka**

Vis didėjantis organinių liuminescencinių medžiagų poreikis optoelektronikos srityje paskatino vystyti tyrimus visame Pasaulyje. Organinės funkcinės medžiagos, pasižyminčios dideliu stabilumu ir tirpumu organiniuose tirpikliuose, labai plačiai naudojamos optoelektroniniuose prietaisuose. Per daugelį metų kumarino dariniai rado pritaikymą optoelektronikoje dėl daugybės savybių, ypač dėl įdomių optinių savybių ir lengvos sintezės. Šiame tyrime kumarino dariniai, savo sudėtyje turintys trifluormetilo grupes, buvo pasirinkti kaip akceptorinė dalis, sujungti su stiprias elektronų donorines savybes turinčiu fenoksazino fragmentu. Buvo suprojektuoti ir susintetinti keturi kumarino pagrindu nauji dariniai su santykinai didelėmis reakcijų išieigomis. Buvo tiriamos įvairios sintezuotų junginių charakteristikos, tokios kaip fotofizikinės, elektrocheminės ir terminės. Junginių terminė analizė atlikta naudojant diferencinės skenuojančios kalorimetrijos ir termogravimetrinės analizės metodus. Nustatyta, kad medžiagos yra termiškai stabilios ir geba formuoti stabilius amorfinius stiklus. Kumarino darinių fotofizikinės savybės buvo tiriamos absorbcijos ir emisijos spektrometrijos metodais. Jie atskleidė panašų fotofizikinį junginių elgesį, o kietų plėvelių fluorescencijos kvantiniai efektyvumai išsidėsto intervale nuo 0,3 iki 0,8. Elektrocheminės savybės buvo ištirtos atliekant ciklinės voltamperometrijos matavimus, kuriu metu nustatyta, kad jonizacijos potencialai visų junginių panašūs (siekia 5,09 eV), ir kurių vertės pakankamai aukštos, junginius pritaikant optoelektroniniuose prietaisuose. Susintetintos medžiagos parodė teigiamą solvatochromizmo efektą naudojant skirtingą poliškumo tirpiklius, patvirtinantį intramolekulinių krūvių pernešimą į junginių struktūras. Taip pat buvo suprojektuota ir pasiūlyta kumarino darinių technologinė linija.

## Table of contents

<b>List of figures .....</b>	<b>8</b>
<b>List of tables .....</b>	<b>9</b>
<b>List of abbreviations and terms.....</b>	<b>10</b>
<b>1. Introduction .....</b>	<b>11</b>
<b>2. Literature review .....</b>	<b>13</b>
2.1. Genesis of organic light emitting diodes .....	13
2.2. Fundamentals of OLED.....	13
2.2.1. Structure of OLED .....	14
2.2.2. Light emitting mechanism in OLED.....	15
2.2.3. Fabrication methods .....	17
2.3. Emitting materials .....	18
2.3.1. Acridine and its derivatives .....	19
2.3.2. Coumarin and its derivatives .....	20
2.4. Orange-red emitters .....	23
2.5. Summary of literature review .....	24
<b>3. Experimental part .....</b>	<b>25</b>
3.1. Instrumentation.....	25
3.2. Materials .....	26
3.3. Methodology.....	27
3.3.1 Synthesis of intermediate compounds.....	27
3.3.2 General procedure for the synthesis of target compounds .....	29
3.4. Results and Discussion .....	32
3.4.1. Design and synthesis .....	32
3.4.2. Thermal properties.....	34
3.4.3. Theoretical studies.....	37
3.4.4. Electrochemical properties .....	38
3.4.5. Photoelectrical properties .....	40
3.4.6. Photophysical properties .....	41
<b>4. Recommendations.....</b>	<b>47</b>
<b>5. Occupational safety and health .....</b>	<b>49</b>
5.1. Characteristic of designed materials.....	49
5.2. Occupational risk assessment .....	49
5.3. Safe production.....	52
5.4. Hygiene standards .....	53
5.5. Fire safety .....	54

## List of figures

<b>Fig. 1.</b> Schematic representation of OLED structure .....	14
<b>Fig. 2.</b> Energy level diagram in OLED .....	15
<b>Fig. 3.</b> Examples of phosphorescent emitters .....	16
<b>Fig. 4.</b> Light generation mechanisms in OLEDs .....	16
<b>Fig. 5.</b> Different emitters representing each light emission method .....	18
<b>Fig. 6.</b> Molecular structures of acridine, <b>DMAc</b> and acridine based emitter, <b>TRZ-DDMAc</b> .....	20
<b>Fig. 7.</b> Molecular structures of coumarin (a) and a coumarin derivative (b) .....	20
<b>Fig. 8.</b> Coumarin compounds having substitutions at 3 and 7-positions .....	21
<b>Fig. 9.</b> Molecular structures of <b>PHzMCO</b> and <b>PHzBCO</b> .....	22
<b>Fig. 10.</b> Red emitters based on phenoxazine ( <b>PXZ-DCPP</b> ) and 2,1,3-benzothiadiazole ( <b>BTZ-DMAC</b> ) .....	23
<b>Fig. 11.</b> Single crystal structure of the compound <b>NS-8a</b> .....	34
<b>Fig. 12.</b> DSC thermograms of <b>NS-5a</b> , <b>NS-8a</b> , <b>NS-9a</b> and <b>NS-10a</b> .....	35
<b>Fig. 13.</b> TGA curves of <b>NS-5a</b> , <b>NS-8a</b> , <b>NS-9a</b> and <b>NS-10a</b> .....	36
<b>Fig. 14.</b> Chemical structures of the target compounds, <b>NS-5a</b> , <b>NS-8a</b> , <b>NS-9a</b> , <b>NS-10a</b> .....	37
<b>Fig. 15.</b> Theoretically calculated HOMO and LUMO levels distributions and optimized geometries of <b>NS-5a</b> , <b>NS-8a</b> , <b>NS-9a</b> , <b>NS-10a</b> DFT calculations were performed at the B3LYP/6-31G (d,p) ...	38
<b>Fig. 16.</b> CV curves of dilute solutions of derivatives <b>NS-5a</b> , <b>NS-8a</b> , <b>NS-9a</b> , <b>NS-10a</b> in dichloromethane (100mV/s) .....	40
<b>Fig. 17.</b> Electron photoemission spectrum of the vacuum solid film of <b>NS-5a</b> , <b>NS-8a</b> , <b>NS-9a</b> , <b>NS-10a</b> .....	41
<b>Fig. 18.</b> Absorption spectra of compounds <b>NS-5a</b> , <b>NS-8a</b> , <b>NS-9a</b> <b>NS-10a</b> in solvents (THF, CHCl <sub>3</sub> , toluene) .....	42
<b>Fig. 19.</b> Photoluminescence spectra of compounds <b>NS-5a</b> , <b>NS-8a</b> , <b>NS-9a</b> , <b>NS-10a</b> in differnt solvents (toluene, CHCl <sub>3</sub> , THF) .....	44
<b>Fig. 20.</b> Absorption and photoluminescence spectra of solid films of compounds <b>NS-5a</b> , <b>NS-8a</b> , <b>NS-9a</b> and <b>NS-10a</b> .....	44
<b>Fig. 21.</b> Technological line for the production of coumarin derivatives <b>NS-5a</b> , <b>NS-8a</b> , <b>NS-9a</b> , <b>NS-10a</b> .....	48



## List of tables

<b>Table 1.</b> Spectroscopic properties of coumarin derivatives .....	21
<b>Table 2.</b> Physical properties of compounds <b>PHzMCO</b> and <b>PHzBCO</b> .....	22
<b>Table 3.</b> Thermal characteristics of the coumarin derivatives, <b>NS-5a, NS-8a, NS-9a, NS-10a</b> .....	34
<b>Table 4.</b> Oxidation potential, ionization potential electron affinity of <b>NS-5a, NS-8a, NS-9a and NS-10a</b> .....	40
<b>Table 5.</b> Photophysical characteristics of the compounds ( <b>NS-5a, NS-8a, NS-9a and NS-10a</b> ) .....	44
<b>Table 6.</b> Comparison of the spectral properties of the researched compounds, <b>NS-5a, NS-8a, NS-9a, NS-10a</b> .....	45
<b>Table 7.</b> Description of materials and its hazardous properties .....	49
<b>Table 8.</b> Standard and lab reading values of physical factors.....	51
<b>Table 9.</b> Working hygiene standards .....	53
<b>Table 10.</b> Occupational exposure limits for chemicals .....	53

## List of abbreviations and terms

Abbreviation	Meaning
AC	Alternate current
DC	Direct current
DCM	dichloromethane
DMAC	9,9-dimethyl-9,10-dihydroacridine
DMF	Dimethylformamide
DSC	Differential scanning calorimetry
EA	Electron affinity
$E_g$	Optical band gap
EQE	External quantum efficiency
HOMO	Highest occupied molecular orbital
ICT	Intramolecular charge transfer
$I_p$	Ionization potential
LUMO	Lowest unoccupied molecular orbital
NMR	Nuclear magnetic resonance
OLED	Organic light-emitting diode
PL	Photoluminescence spectroscopy
PLQY	Photoluminescence quantum yield
TADF	Thermally activated delayed fluorescence
$T_{cr}$	Crystallization temperature
$T_d$	5% weight loss decomposition temperature
$T_g$	Glass transition temperature
$T_m$	Melting point
TGA	Thermogravimetric analysis
TLC	Thin layer chromatography
TMS	Tetramethyl silane
UV-Vis	Ultraviolet-visible spectroscopy

## 1. Introduction

Electroluminescent organic materials play an important role in the field of organic optoelectronics. Recent upgrades of functional materials made the organic devices like organic light-emitting diodes (OLEDs), organic semiconductor lasers, organic solar cells (OSCs), organic sensors, organic memories, organic transistors and integrated devices, an imperative part of the commercial and academic domain [1]. OLEDs have impacted in such a way that they could be found as primary options for energy-efficient solid-state lighting and display devices. This is fundamentally because of the simple variations that could be done in material properties making it multi-faceted [2,3]. The applications could be attributed to its features such as self-emission, flexibility, color purity and less power consumption. Eventhough it has constraints pertaining to life-time and efficiency, the benefits of OLEDs far exceeds [2,3].

An OLED is an electroluminescent device, that consists of multiple organic layers placed in between two electrodes. For the effective functioning of OLEDs, careful selection of organic conductive materials applied in the device is imperative [3]. In view of the wide span OLED applications, the functional layers has to be designed in a manner capable to meet the requirements desired. Modulation of emission wavelength could be acquired by appropriate fabrication of fluorophore scaffold. This indeed is the meritorious aspect of OLEDs in display market. Further, to control color and efficiency of organic luminescent device, appropriate electron donors and acceptors should be incorporated on the molecular skeleton [4].

The materials applied in the device could be either small molecules or polymers. Generally, organic compounds such as carbazole, acridine, triphenylamine and anthracene are opted for scientific investigations. Most of the other electroactive materials are not exploited which might be eligible for OLEDs [3]. In this contribution, variants of coumarin are particularly given attention as electroluminescent material. Coumarin and its derivatives are known to possess electron-withdrawing ability and are widely used as fluorescent dyes. However, only few researches are focussed on applicability of coumarins in OLEDs. The striking features of coumarin are its good thermal stability and optical properties, which are quite essential for productive device operation. In addition to that, the relative ease of its synthesis is yet another attractive feature [5,6]. In this context, coumarin based derivatives were designed and synthesized in this work. The coumarin variants used has strong electron-withdrawing trifluoromethyl groups as substituents at different positions [7].

The electroactive materials developed in the present work are focussed to attain orange-red emission. There are still few reports on coumarin derivatives with orange-red emission since most synthesized coumarin derived forms have blue-green emission. To design the target molecules, phenoxazine was introduced as donor unit. With phenoxazine, there are the merits of its structure which can aid efficient HOMO-LUMO separation and possess rigid molecular structure. Further, strong charge transfer states and stiff molecular framework are recommendable for long-wavelength emission. Therefore, incorporation of phenoxazine moiety could fulfill these criterions for orange-red emitters [8,9]. In view of the above mentioned findings, the present work combined coumarin-derived moieties with phenoxazine to afford new promising entities for optoelectronic applications.

**The main task of the work:** synthesis and studies of properties of derivatives of coumarin-based compounds for organic light emitting devices.

**The tasks proposed to achieve the aim:**

1. Synthesis and characterization of coumarin based compounds having trifluoromethyl fragments.
2. Study of the thermal, photophysical, electrochemical and photoelectrical properties of the obtained products.
3. Development of a technological scheme for the production of the synthesized compounds.

## **2. Literature review**

A comprehensive assessment was carried out on the research topic and is provided in the section below. This review mainly consists of four segments, of which the first section is briefly about the development of organic light emitting diodes. Following which, the concepts of OLEDs and the various photophysical mechanisms employed for light generation are emphasized in the second segment. Furthermore, the third segment covers some of the electroactive materials utilised for creating emissive layer in OLEDs, that contributed to the development of target molecules. The final segment sheds light on long wavelength emission materials.

### **2.1. Genesis of organic light emitting diodes**

Even before OLED technology evolved, people were employing different kinds of display and lighting technologies. The most initial and prominent one was incandescent lamps, developed by Edison in 1870. Although in 1922, cathode ray tube (CRT) was developed, it also had similar limitations as found in incandescent lamps (e.g. bulkiness and inefficiency). Over the years from 1930 to 1962, several lighting and display technologies like fluorescent lamps, inorganic light emitting diodes (LEDs) and liquid crystal displays (LCDs) were developed. Among these newly developed technologies, LCD technology had noteworthy impact on the display domain. Besides the exceptional features of LCD, it faced challenges related to flexibility, viewing angle and response time. The flaws pertaining the above mentioned technologies prompted further study on more efficient and compatible alternative technology in optoelectronics [2].

The discovery of OLED technology in 1987 marked a milestone in the long researched sector of optoelectronics. This was found by two chemists in Eastman Kodak company, Ching.W.Tang and Steven Van Slyke [10]. Ever since then, continuous improvements are done through profound studies across the world. OLEDs are pliable, energy efficient and its fabrication is simple. It does not require back-lighting as it emits its own light, have faster response time and provide better viewing angle, when compared to LCDs [11]. However, the brief functioning period and its sensitivity to water and UV make it an evolving research area.

### **2.2. Fundamentals of OLED**

OLEDs are electroluminescent devices based on organic materials that emit light in response to electric current. The process of electroluminescence that occurs in an organic LED is controlled by the spectral properties of the active elements, device structure and electrical properties of the conducting layer. Once an appropriate voltage is applied to the OLED, current flows through the device. The electrons are generated by cathode and holes by anode. In the emissive layer, the electrons and holes recombine to form exciton to give off light. The recombination occurs either by singlet-singlet transition or singlet-triplet transition giving out their energy as photons [2,11]. The light emission is not a direct consequence of recombination of electrons and holes. At first, an excited molecule called exciton is formed, while emanating light. Thus, simultaneous deactivation to ground state occurs. The binding energy is the feature that describes the exciton, as more excitons would be localized when the binding energy is high. For effective electron-hole recombination, an equivalence or equity is preferred between the electron and hole flux. In electroluminescence, the introduction of electrons is the main controlling step in the whole process [12].

### 2.2.1. Structure of OLED

Initially, OLEDs were made up of a single organic layer placed in between electrodes. This gradually developed to multiple layers, which enhanced the device output [3]. The typical structure of multi-layer OLEDs consists of a cathode, electron transport layer, emissive layer, hole transport layer, hole injection layer and an anode.

- Base: The base on which all layers are placed is called substrate and consists of glass or metal foils or semiconductor or plastic materials.
- Anode: The electrode with the positive charge is called anode. Materials with high work function and conduction like ITO should be used for anode.
- Hole Transport layer: Hole transport layer helps to carry the holes while preventing electrons from coming to the opposite electrode.
- Electron Transport layer: electron transport layer helps to carry electrons and prevents holes coming to the opposite electrode.
- Cathode: Cathode is the electrode with negative charge. Generally, materials with low work function like calcium and magnesium are used for making this electrode [2].
- Emissive layer: The most important coating is the emitting layer. The emissive layer consists of luminescent materials, where the charges combine to emit light. The color of the light given out is regulated by the difference in energy levels of HOMO and LUMO of emissive layer. Thus a suitable layer has to be found for modulating the color of emission from the visible region. The given supply of electric current decides the intensity of the emitted light. The efficiency of OLED could be improved either by altering the thickness of layers or by incrementing doping concentration of layers [2]

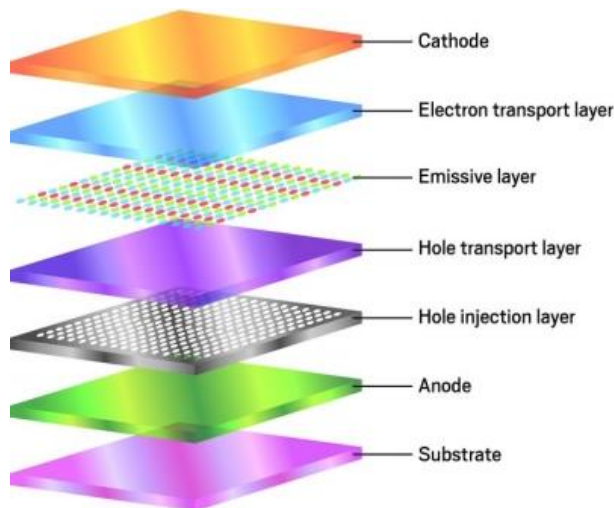


**Fig. 1.** Schematic representation of OLED structure [13]

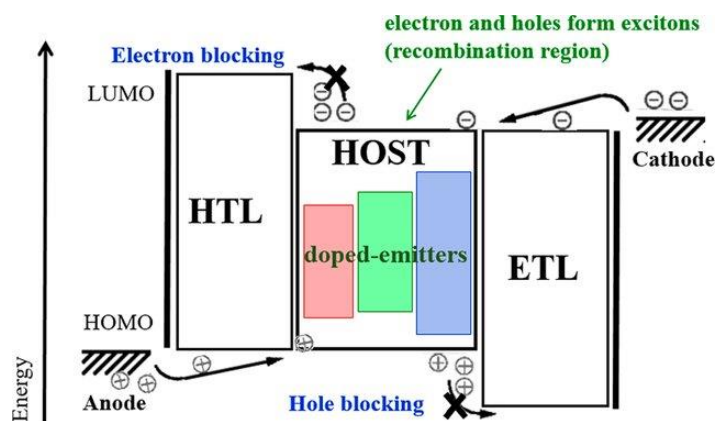


Fig. 2. Energy level diagram in OLED [14]

### 2.2.2. Light emitting mechanism in OLED

The principal luminescence process used in OLEDs earlier was fluorescence. Basically, only singlet excitons could be utilized for emission in a radiative form, whereas the energy of most of the triplet excitons gets exhausted in a non-radiative manner as heat [15]. In fluorescence, radiative transition of singlet excitons occurs from lowest singlet excited state ( $S_1$ ) to the ground state ( $S_0$ ). This happens instantly and has small lifetime in the range of nanoseconds. According to spin statistics, the 75% excitons found in OLED are in triplet state. Thus, fluorescent OLEDs have only internal quantum efficiency (IQE) of 25% with external quantum efficiency of 5% [15]. Internal quantum efficiency is the ratio of photons generated to produce electroluminescence to the applied current [1]. Among the salient criteria required, external quantum efficiency (EQE) has been indispensable for productive performance of an organic electroluminescent device [16].

The drawback of fluorescent OLEDs in employing the 75% triplet excitons for emission instigated the pursuit for a more efficient mechanism. In 1998, Baldo et al. displayed phosphorescence for electroluminescence using metal complexes such as platinum. In phosphorescence, both singlet and triplet excitons were used for emission. Further developments in phosphorescence led to higher performing electroluminescent devices using metal complexes such as osmium, iridium [15]. The spin orbit coupling between the exciton spin angular momentum and the orbital angular momentum becomes more by the influence of heavy metals. Radiative decay from the triplet state ( $T_1$ ) to the ground state singlet ( $S_0$ ) arises as a consequence of spin orbit coupling. Furthermore, spin orbit coupling assists intersystem crossing between the  $S_1$  and  $T_1$ , increasing the triplet excitons (shown in Figure 4). OLEDs with this kind of mechanism have internal quantum efficiency 100% and are known as second generation OLEDs [17]. However, several demerits were found in the utilization of phosphorescent emitters. Some of them are that the metal complexes used were rare earth metals having lesser availability, toxic in nature and expensive [15]. Among the metal complexes designed for organic luminescent devices, a few instances are given below:

- *tris*(2-phenylpyridine) iridium ( $\text{Ir}(\text{ppy})_3$ ): a green emissive material.
- bis[2-(2-pyridinyl-*N*)phenyl-C](acetylacetonato)iridium(III) ( $\text{Ir}(\text{ppy})_2(\text{acac})$ ): green emitter.
- *tris*(1-phenylisoquinoline)iridium(III) ( $\text{Ir}(\text{piq})_3$ ): red phosphorescent material.
- bis[2-(5-cyano-4,6-difluorophenyl)pyridinato- $C_2,N$ ]iridium(III): blue emitter.

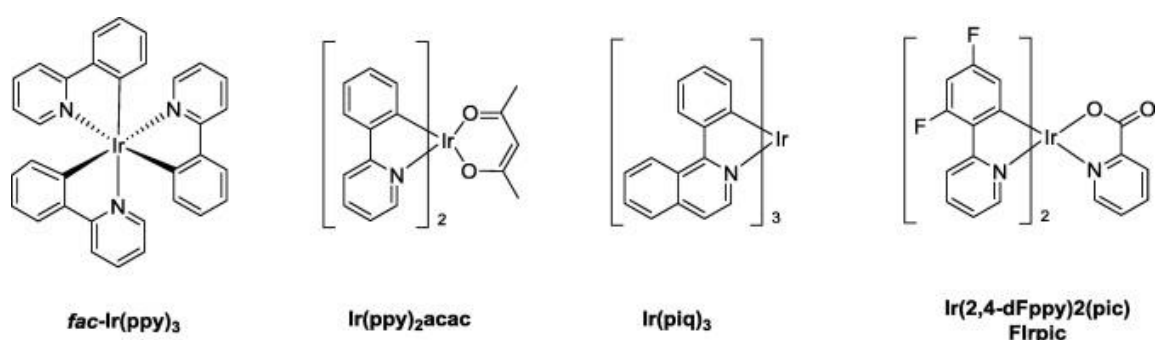


**Fig. 3.** Examples of phosphorescent emitters [18]

The shortcomings of phosphorescent OLEDs stimulated researchers in the quest for an alternative or an efficient mechanism with 100% internal quantum efficiency with large external quantum efficiency. The quest resulted in fluorescent emitters exhibiting thermally activated delayed fluorescence (TADF).

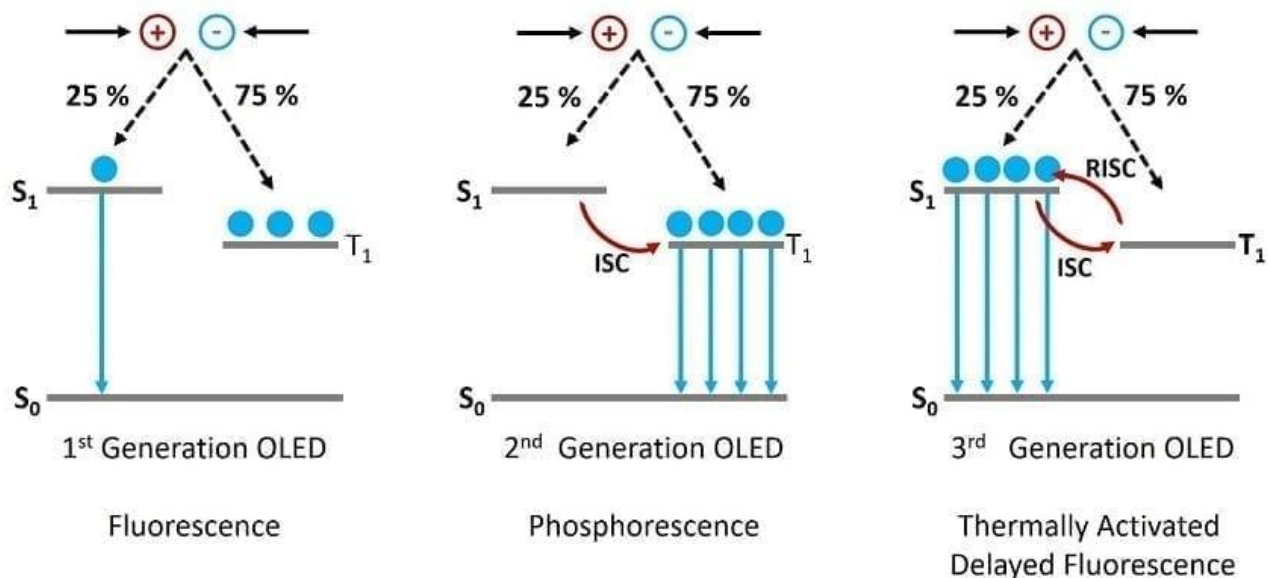


**Fig. 4.** Light generation mechanisms in OLEDs [17]

Although the idea of TADF was originally stated by Perrin et al. in 1929, it was Chihaya Adachi in 2012 for the first time used thermally activated delayed fluorescence in OLED. Since then it became the central theme of researchers around the world [17]. Adachi used this mechanism in pure organic molecules for attaining desirable quantum efficiencies. The TADF mechanism is controlled by the difference between the HOMO-LUMO in a molecule. TADF materials can garner both singlet and triplet excitons by reverse intersystem crossing (RISC), thus reaching 100% IQE conceptually. For the upconversion of lowest triplet excitons (T<sub>1</sub>) to the lowest singlet excitons (S<sub>1</sub>), the difference in energy or the energy gap between these states should be less (about <0.1 eV) [15].



The TADF molecule is designed in such a way that its energy gap ( $\Delta E_{st}$ ) is lesser than a typical organic entity. With smaller energy gap, reverse intersystem crossing occurs, where the excitons in the  $T_1$  levels are changed to  $S_1$  levels by thermal activation. After the excitons are in the  $S_1$ , they could easily transition to  $S_0$  by fluorescence. As RISC occurs slowly, fluorescence by triplet excitons is produced much later than the fluorescence produced by the excitons created in the  $S_1$  levels. As a consequence, this method is known as E-type delayed fluorescence [17]. Usually two types of photoluminescence could be observed in TADF emitters, prompt fluorescence and delayed fluorescence. The singlet excitons when emit radiatively result in prompt fluorescence and occurs within nanoseconds. In delayed fluorescence, emission is the result of intersystem crossing to the triplet state followed by RISC causing singlet state repopulation. Delayed fluorescence happens within the range of milli to micro seconds [17].

Several other complicated exciton harvesting mechanisms were reported, generally called bimolecular or trimolecular emitting mechanism. They are P-type delayed fluorescence or triplet-triplet annihilation, hyperfluorescence, exciplex emission and exciplex-assisted emission [19]. The key factor required for the design of TADF emitters is small energy gap. In order to attain smaller energy gap, detachment of relevant transition orbitals is needed. This separation causes charge transfer transition from HOMO to LUMO, which in turn improves RISC [8]. Designing a molecule by using electron donating (donor) and electron withdrawing (acceptor) moieties could bring about a charge transfer structure with constrained HOMO and LUMO orbitals. This could be enhanced by increasing the twist angle between the donor and acceptor parts. Nevertheless, for RISC to occur a slight overlap of the orbitals is required. Thus a balance between small energy gap and overlap has to be achieved [20]. Another requirement for TADF molecule is high photoluminescence quantum yields (PLQY) along with short excited state lifetimes. This will make certain to have effective RISC and radiative decay from the singlet state.

### **2.2.3. Fabrication methods**

For the manufacture of OLEDs, deposition of organic layers to the substrate is the most important part [11]. The most generally used OLED device fabrication techniques are vacuum thermal evaporation and solution processing. Devices which are thermally evaporated manifest large performance as they can form even and regular films. But other solution methods like spin coating, screen printing or ink-jet printing are considered promising for large scale production as their fabrication is relatively simple and economical. The small molecule based devices are fabricated using both solution and vacuum evaporation whereas dendrimers and polymers based devices by solution processes [15].

### 2.3. Emitting materials

Many investigations have reported numerous materials for light emission. Electroluminescent materials used in the emitting layer could be divided mainly into two groups, small molecules and light-emitting conjugated polymers. Some of the primary popular light-emitting polymers are polyacetylene, polypyrrol, polythiophene *etc.* [21]. The limitation of OLEDs regarding the use of expensive noble metals like iridium and platinum was resolved by the emergence of organic luminescent materials displaying fluorescence, phosphorescence or TADF [1]. An efficient emission is the result of effective injection of electrons and holes. Thus, electroluminescent molecules should have appropriate HOMO/LUMO energy levels alongwith high quantum efficiency, fine film-forming characteristics and should be thermally stable [22]. To sum it up, the overall performance of OLEDs heavily depend on the materials used for emitting layer.

The energy gap ( $\Delta E_{st}$ ) of organic fluorescent molecules were found to be comparatively big. As 75% of the excitons produced are dissipated as heat energy during emission, only 25% singlet excitons are effectively used. Among the many fluorophores, aluminium *tris*-(8-hydroxyquinoline) ( $Alq_3$ ) is a classic emitter used in OLED. Unlike fluorophores, phosphorescent molecules have relatively bigger  $\Delta E_{st}$  [19]. Phosphorescent materials have the ability to exploit both the triplet and singlet excitons with the help of heavy atoms, leading to 100% efficiency. However, owing to its unstability and high-cost, phosphorescent dyes faced challenges [23]. TADF molecules make use of all the excitons available maximizing the efficiency of OLEDs. Derivatives of eosin, fullerene and porphyrin are widely known materials that display E-type delayed fluorescence. Initially, TADF mechanism was regarded to possess low power conversion efficiency due to its heat absorbing nature. Over the time it has been proven that efficiency could be enhanced by proper designing of TADF molecules [1].

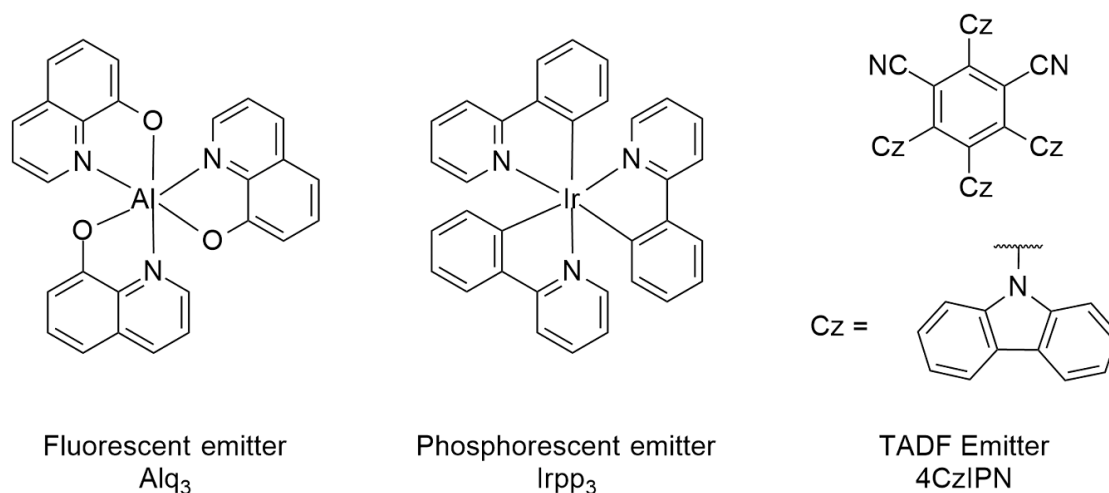


**Fig. 5.** Different emitters representing each light emission method [19]

Although both small molecules as well as polymeric molecules are employed in the present day OLEDs, small-molecule emitters are found to be more superior. One of the reasons for their superiority is because they form a dynamic constituent in equivalent polymeric materials [23].

TADF emitters are designed in such a way that they contain both donor and acceptor moieties. In which nucleophiles are used as donor moiety in order to promote hole transport through oxidation

while electron accepting moiety is formed using electrophilic molecules. The donor and acceptor moieties influences the color of the resultant TADF molecule. The type of donor used have an impact on the HOMO and the acceptor unit dominates LUMO. The color emitted from the molecule depends on the energy band gap. Furthermore, the design of the connectivity between donor and acceptor alters the overlaps between HOMO and LUMO [19]. The typically utilized donor unit in most of the research works are carbazole, triphenylamine, acridine, phenoxazine and phenothiazine [24]. In most cases, researchers use substituents to alter the features [25]. For the construction of D-A type TADF molecule, numerous kinds of electron withdrawing molecules are employed. They affect the major attributes of TADF emitter like period of excitation, emission wavelength and efficiency. Some of them are cyano-substituted aromatics, triazine, diphenyl sulfoxide and benzophenone-based groups [26].

### 2.3.1. Acridine and its derivatives

Acridine was separated from coal tar by Graebe and Co in 1870 [27]. Acridines are a prominent class of heterocyclic systems that have nitrogen, due to its plethora of essential qualities. Acridine derivatives could be seen in plants and marine organisms. Derivatives of acridine are known to possess distinctive physical and chemical traits, biological and industrial usages. For more than two centuries, it has found applications in dyes and pigments sector. It has several features in pharmaceutical industry like anti-bacterial, anti-cancer, anti-inflammatory, anti-microbial and anti-malarial. In addition to that, acridines find applications in fluorescent materials and laser technologies. Its semi-planar heterocyclic structure and inter-molecular interactions contribute to its variety of characteristics particularly chemiluminogenic [28].

To obtain acridine derivatives, various synthetic strategies are developed. Out of which, ring closure mechanism is found to be efficient. In ring closure reaction, the aromatic ring is customised with apt substituent for the required derivative. Other techniques used are oxidation, reduction and rearrangement [27]. One of the plus points of acridine derivatives is that easy amendment is possible. Other strong factors for their applicability are their good thermal stability and triplet state energy. Since it is an established compound, acridine compounds are slightly expensive [27].

The most common acridine derivative used is 9,9-dimethyl-9,10-dihydroacridine (**DMAC**). It forms the building unit of a number of organic materials that functions as emitter, hole-transporting molecule and host material in organic devices (structure of it is depicted in Figure 6.). Another derivative, 9,9-dimethyl-10-phenyl-9,10-dihydroacridine (**PhDMAC**) was developed as TADF emitter by Adachi et al. [27]. Figure 6 depicts the structure of acridine, its derivative **DMAC** and an emitter based on acridine.

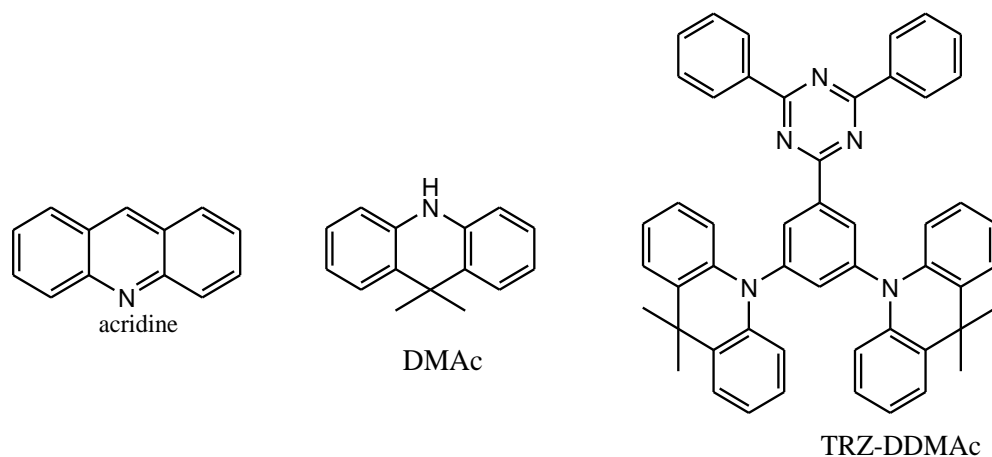


**Fig. 6.** Molecular structures of acridine, **DMAc** and acridine based emitter, **TRZ-DDMAc**

### 2.3.2. Coumarin and its derivatives

Coumarin (*2H*-chromen-2-one) belong to the chemical class of benzo- $\alpha$ -pyrones. They are made by the combination of  $\alpha$ -pyrone and benzene ring [29,30]. Its identification could be traced back to 1820 from tonka bean by A. Vogel [29]. Coumarin compounds are an array of interesting and multifunctional molecules. Their diverse kind of applications involve manufacture of drugs, perfumes, fluorescent brightening agents, colorants, lasers, solar cells, optical storage devices, *etc.* Apart from their biological functions, on account of their intrinsic photochemical properties, good solubility and stability, they have formed a niche in electronics and photonics sector [5,6,29,30,31].

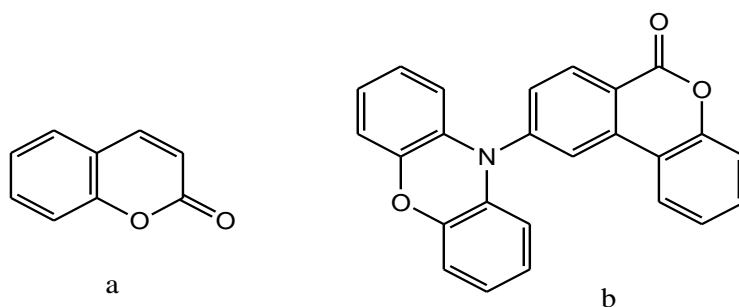


**Fig. 7.** Molecular structures of coumarin (a) and a coumarin derivative (b)

The substituent connected to the coumarin ring has considerable impact on the light emission characteristics of the coumarin derivative. High fluorescence could be observed depending on the type of substituent at different positions [5,30,31]. Furthermore, suitable substitution prompts intermolecular charge transfer, which in turn results in intense fluorescence from derivatives of coumarin [32].

Studies conducted on relation between coumarin scaffold and addition of functional groups have suggested this. In one such case study they attached electron-rich diethylamino at the 7-position and an electron-deficient ethoxy carbonyl group to the 3 position of coumarin moiety . As a consequence,

the quantum yield ( $\phi_f = 0.001-0.81$ ) rose significantly while prominent redshifts were observed in the maximum emission and absorption spectra (89 nm and 149 nm) [32, 33]. The effect 3- and 7-substitution on photophysical characteristics is given in the Table 1. Coumarins with acceptor at 3-position and donor at 7-position are depicted in the Figure 8.

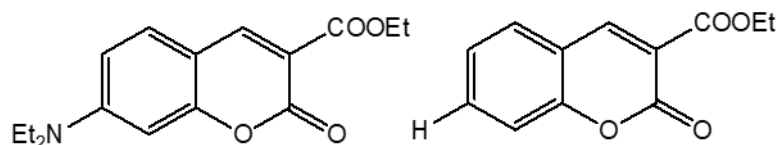


**Fig. 8.** Coumarin compounds having substitutions at 3 and 7-positions

**Table 1.** Spectroscopic properties of coumarin derivatives [32, 33]

3-A <sup>1</sup>	7D <sup>1</sup>	$\lambda_{\text{abs}}, \text{nm}$	$\lambda_{\text{em}}, \text{nm}$	$\Phi_f$
H	H	330	380	0.002
H	NEt <sub>2</sub>	373	440	0.73
COOEt	H	334	415	0.12
COOEt	NEt <sub>2</sub>	412	529	0.81

<sup>1</sup> 3-A= acceptor at 3-position, 7-D = donor used at 7-position

Reports state that 3- and 7-substitution of coumarins with functional groups such as amino, hydroxy and methoxy could result in changes in the color and fluorescence features. In particular, altering the electron-accepting ability through substitution at 3-position of coumarin has excellent outcomes in absorption and emission properties. Cyanocoumarins are regarded as prospective building blocks for nitrogen containing cyclic compounds. Besides substitution, thermal stability of the materials is regarded to be a parameter of prime importance. This is because thermal stability of organic molecules could improve the stability and lifetime of devices [5]. Based on latest developments, orange color emitting coumarin analogues has been realized by regulating absorption wavelengths from 300 nm to 550 nm [32].

The conventional synthesis strategies employed for preparing coumarins are Knoevenagel condensation, Pechmann, Perkin, Claisen rearrangement, Wittig and Reformatsky reactions. Different compounds are used as starting materials for obtaining coumarin and its derivatives, like aldehydes, phenols, ketones, carboxylic acids. The yield of the product depends on the selection of the type of method and material. Among the various synthetic reactions used, Knoevenagel condensation is known to be the most prevalent and uncomplicated process [5,34].

Interestingly, in the 20th century, 3-(2-benzothiazolyl)-7-diethylamino coumarin was investigated to be an effective light emitting material in OLED by Tang and coworkers. This in turn triggered studies on coumarin analogues [35]. Over the years, different groups of researchers have found coumarin derivatives with comparatively stronger photoluminescence quantum yield. Recent reports include those by Patil et al., in which they described synthesis of a coumarin based luminescent material, 7-(9H-carbazol-9-yl)-4-methyl coumarin. Further, they reported it to possess good PLQY of 0.70 and had success when employed in OLED for deep blue color with doped matrix [35].

Later in 2017, a team by Jia-Xiong Chen reported two coumarin derivatives, 3-methyl-6-(10*H*-phenoxazin-10-yl)-1*H*-isochromen-1-one (**PHzMCO**) and 9-(10*H*-phenoxazin-10-yl)-6*H*-benzo(*c*)-chromen-6-one (**PHzBCO**) as TADF emitters [35]. They observed moderately high PLQYs in these materials of about 0.47 and 0.52. The materials had smaller  $\Delta E_{st}$  of 0.018 and 0.006 and their EQEs were relatively good of about 17.8% and 19.6%, respectively. All these made them favourable to be used as TADF emitter in OLED. The photophysical and energy level values from this research are given in the Table 2 [35].

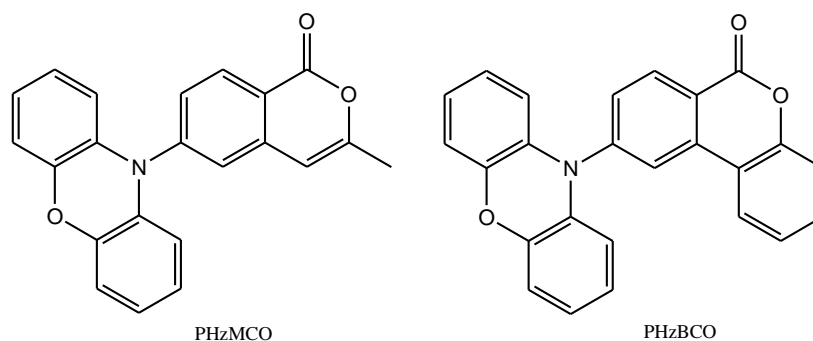


**Fig. 9.** Molecular structures of **PHzMCO** and **PHzBCO**

**Table 2.** Physical properties of compounds **PHzMCO** and **PHzBCO** [35]

	$\lambda_{abs}$ , (nm)	$\lambda_{em}$ , (nm)	$\Delta E_{st}$ , (eV)	PLQY	HOMO(eV)	LUMO(eV)
<b>PHzMCO</b>	320/395	510	0.018	0.47	-5.28	-2.86
<b>PHzBCO</b>	306/395	524	0.006	0.52	-5.24	-2.97

The photophysical characterization was derived from UV-Vis absorption and emission spectra in toluene solution ( values given in the Table 2). Wide absorption was observed for both materials (366-450 nm). The  $\Delta E_{st}$  values measured from the fluorescence spectra was agreeing with the values deduced using DFT calculations. The values got from theoretical calculations of  $\Delta E_{st}$  pointed out that the materials obtained were capable of effective RISC. The HOMO and LUMO values were estimated by the authors by use of onset oxidation and reduction potential against ferrocene [35]. The energy levels of **PHzBCO** were smaller which could be the effect of conjugation induced by the phenyl ring and was investigated as emitter on OLED device. The maximum power efficiencies were 52.07 cd/A and 61.23 cd/A, respectively. The maximum current efficiencies were 48.01 lm/W and 60.09 lm/W, respectively. The electroluminescence spectra of the two derivatives showed green emission maximum at 508 and 520 nm. There was slight difference in the EL spectra inferring fine stability of emission [35].

In solid state, coumarin analogues has a tendency for self-quenching as a consequence of intermolecular forces and aggregation. This could explain the lesser choice of coumarin derivatives as material for light emitting layer in OLEDs. At present, they are exploited as dopants in host materials of OLEDs [36].

Taking into account all its pros and cons, coumarin-derived compounds possess good luminescent attributes, which offer them prospects in OLED.

## 2.4. Orange-red emitters

The red electroactive materials are a significant part of white OLED fabrication. The number of efficient red organic emitters is lesser when compared to green or blue emitters. This is due to hindrances faced in tailoring effective molecules and acquiring appropriate device efficiency. One of the challenges is that, orange-red emitters undergo high internal conversion by energy gap law, which in turn results in exciton decay. On account of this, it is observed that red emitters are likely to show low PLQY in comparison to other emitters. Red emission could be realized through developing strong polar or non-polar  $\pi$ -conjugated framework. Thus, rigid molecular backbone structure along with strong charge transfer states in electron donor-acceptor (D-A) system forms the solution for building efficient orange-red emitters [23,37]. Some examples of red emitters are shown in the Figure 10.

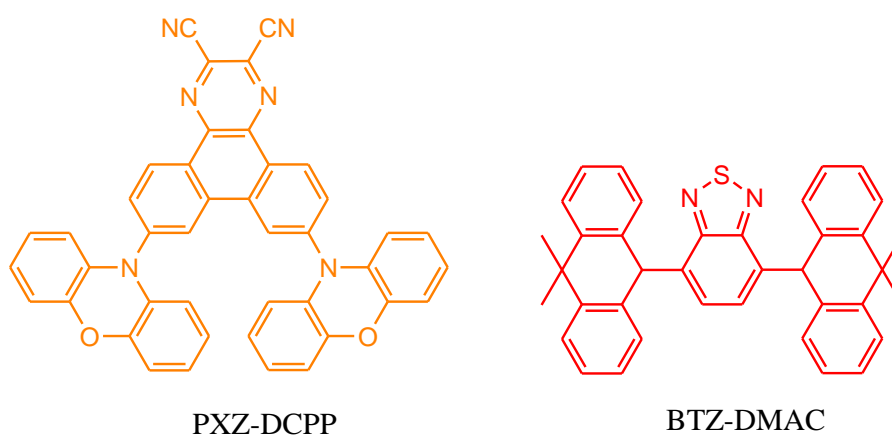


**Fig. 10.** Red emitters based on phenoxazine (**PXZ-DCPP**) and 2,1,3-benzothiadiazole (**BTZ-DMAC**)

Several reviews and reports have brought to light molecules prepared for red emission, with electron-withdrawing units such as 2,1,3-benzothiadiazole, 2,3-dicyanopyrano phenanthrene (**DCPP**) along with electron-donating segments like carbazole, acridine, phenoxazine and phenothiazine [23]. The research group by Binyan Wang suggested a compound built using phenoxazine and 2,3-dicyanopyrazino phenanthrene moieties (**PXZ-DCPP**) to be relatively efficient orange-red emitter.

This derivative demonstrated good thermal stability with decomposition temperature  $T_d = 355$  °C and implied the possibility for it to form amorphous thin film ( $T_g = 155$  °C). Accordingly, making it a potential candidate for OLED application. An orange light-emitting diode embedded with this material was fabricated. The device with **PXZ-DCPP** displayed high EQE values of 17.4% with maximum power efficiency of 27.8 lm/W. Its turn-on voltage was 3.2V. The electroluminescence spectrum exhibited emission maximum at 608 nm [38].

Derivatives based on 2,1,3-benzothiadiazole was designed and characterized by Yang and coworkers for red emission. Among the derivatives prepared by them, only the sample with dimethylacridine moiety (**BTZ-DMAC**) proved effective. The device employed with this derived compound demonstrated EQE of 8.8% with red emission maximum at 636 nm [23].

## **2.5. Summary of literature review**

Overall, analogues of coumarins are a less explored domain in OLED applications. The data analysed in the previous sections give an insight into the potential utility of these materials in optoelectronic devices. Coumarins and its derivatives have excellent properties and it could be synthesized rather in a simple way. So far, a greater fraction of coumarins designed exhibit blue-green emission. It is desirable therefore to find new derivatives which have longer wavelength emissions. Meanwhile, the red emission could be possible by designing a scaffold with both strong donor and acceptor. Since coumarin moiety is a renowned electron-accepting group, it was preferred as acceptor unit for the multi-functional materials prepared in this study. As for donor unit, phenoxazine was chosen as it is a widely known electron-rich moiety.



### **3. Experimental part**

#### **3.1. Instrumentation**

##### **Nuclear Magnetic Resonance**

$^1\text{H}$  and  $^{13}\text{C}$  nuclear magnetic resonance (NMR) spectra were obtained using *Bruker Advance* spectrometer (400 MHz). For sample preparation, about 20 mg of the product has to be dissolved in the solvent used. Three of the materials were dissolved in deuterated chloroform ( $\text{CDCl}_3$ ) and the other in deuterated dimethyl sulfoxide (DMSO). The spectra is reported as chemical shifts ( $\delta$ ) in ppm with reference to Tetramethyl silane (TMS). The excitation of  $^1\text{H}$  nuclei was by applying a frequency of 400 MHz and of  $^{13}\text{C}$  nuclei by 101 MHz.

##### **Infrared spectroscopy (IR)**

The IR spectra were recorded using *Perkin Elmer Spectrum GX II* in KBr pellets. The infrared spectra are a plot of measured infrared intensities against frequencies.

##### **Mass spectrometry (MS)**

*Waters ZQ 2000* mass spectrometer was used for obtaining mass spectra. Dilute solutions of the materials were made for preparing the samples and are ionized using electrospray ionization. Mass spectra is represented as peak intensity versus mass to charge ( $m/z$ ) ratio (which reflects the mass number).

##### **UV-VIS Absorption Spectroscopy**

The absorption spectra of the compounds diluted in solvents ( $10^{-4}$  M) Tetrahydrofuran (THF) and chloroform ( $\text{CHCl}_3$ ) were recorded using *Perkin Elmer lambda 35* spectrophotometer in quartz cells.

##### **Photoluminescence Spectroscopy**

*FLS980 Fluorescence Spectrometer* manufactured by *Edinburgh Instruments*, was used for obtaining PL-spectra of  $10^{-5}$  M solutions of the compounds. Drop casting technique was applied for the preparation of thin films of the samples from 1 mg/ml solution in different solvents.

##### **Thermogravimetric Analysis (TGA)**

TGA measurements were recorded using *Mettler TGA/SDTA851e/LF/1100*. The heating rate employed was 20 °C/min under nitrogen atmosphere.

##### **Differential Scanning Calorimetry (DSC)**

DSC measurements were carried out on a *DSC Q100 TA* instrument. The analysis was done at a heating rate of 10 °C/min under nitrogen atmosphere.

##### **Electron Photoemission Spectrometry**

The ionization potentials ( $I_p$ ) of the vacuum deposited films of the final products was acquired using photoelectron emission spectrometry in air. A negative voltage of 300 V was given to the sample substrate. Monochromatic light required for the experimental setup was provided using a deep UV

deuterium light source ASBN-D130-CM and CM110 1/8m monochromator. The photocurrent produced on illumination was measured on an electrometer 6517B *Keithley* [3].

### Cyclic Voltammetry

CV measurements were done with a AUTOLAB potentiostat. The electrolyte used for the measurements was 0.1 M solution of tetrabutyl ammonium hexafluorophosphate in dichloromethane. The measurement of potentials were carried out using a three-cell electrode in which carbon as working electrode, platinum wire as counter electrode and silver wire as reference electrode (calibrated against ferrocene/ferrocenium couple) [3].

### X-Ray Crystallography

The crystals were grown using slow evaporation method. The crystallographic analysis was performed on a XtaLAB Mini diffractometer (two-circle diffractometer, CCD plate detector, omega scans, graphite monochromator with Enhance (Mo) X-ray source ( $\lambda = 0.710 \text{ \AA}$ ). The structures were refined using the software package SHELXL. The measurements were done at 293 K. All non-hydrogen atoms were refined anisotropically and all hydrogen atoms were refined isotropically.

### 3.2. Materials

All the reagents were purchased from the suppliers and used without any further purification.

<b>Compounds</b>	<b>Chemical formula</b>	<b>Producer</b>
5-Bromosalicylaldehyde	$C_7H_5BrO_2$	Sigma Aldrich
3-(Trifluoromethyl)phenyl acetonitrile	$CF_3C_6H_4CH_2CN$	Flurochem
4-(Trifluoromethyl)phenyl acetonitrile	$CF_3C_6H_4CH_2CN$	Flurochem
2-(Trifluoromethyl)phenyl acetonitrile	$CF_3C_6H_4CH_2CN$	Flurochem
3,5-Bis(trifluoromethyl)phenyl acetonitrile	$(CF_3)_2C_6H_3CH_2CN$	Flurochem
Piperidine	$(CH_2)_5NH$	Sigma Aldrich
Acetic Acid	$CH_3COOH$	Sigma Aldrich
Palladium(II) acetate	$C_4H_6O_4Pd$	Sigma Aldrich
Tri- <i>tert</i> -butylphosphine (1.0 M in toluene)	$C_{12}H_{27}P$	Sigma Aldrich
Sodium <i>tert</i> -butoxide	$C_4H_9NaO$	Sigma Aldrich
10 <i>H</i> -Phenoxazine	$C_{12}H_9NO$	Sigma Aldrich
Dimethylformamide	$C_3H_7NO$	Sigma Aldrich
Toluene	$C_7H_8$	Sigma Aldrich
Hexane	$C_6H_{14}$	Sigma Aldrich

Ethyl Acetate	C <sub>4</sub> H <sub>8</sub> O <sub>2</sub>	Sigma Aldrich
Sodium sulfate	Na <sub>2</sub> SO <sub>4</sub>	Sigma Aldrich
Acetone	C <sub>3</sub> H <sub>6</sub> O	Sigma Aldrich
Acetonitrile	C <sub>2</sub> H <sub>3</sub> N	Sigma Aldrich
Silica Gel	SiO <sub>2</sub>	Sigma Aldrich
Chloroform	CHCl <sub>3</sub>	Sigma Aldrich
Dimethyl sulfoxide	C <sub>2</sub> H <sub>6</sub> OS	Sigma Aldrich

### 3.3. Methodology

A two-step procedure was applied in obtaining the final products. The four target compounds **NS-5a**, **NS-8a**, **NS-9a**, **NS-10a**, were obtained through palladium catalysed C-N coupling reactions of coumarin derivatives **NS-5**, **NS-8**, **NS-9**, **NS-10**. The intermediate materials **NS-5**, **NS-8**, **NS-9**, **NS-10** were formed by means of condensation of 5-bromosalicylaldehyde with appropriate acetonitriles.

#### 3.3.1 Synthesis of intermediate compounds

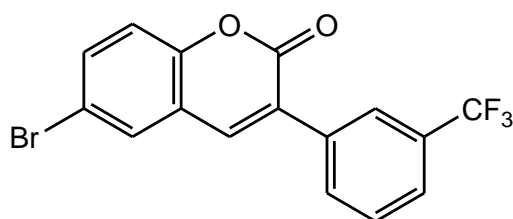
The intermediate compounds **NS-5**, **NS-8**, **NS-9**, **NS-10**, were prepared by following the similar procedure found from the literature source [38].

##### *6-Bromo-3-(3-(trifluoromethyl)phenyl)-2H-chromen-2-one (NS-5)*

5-Bromosalicylaldehyde (1 g, 4.97 mmol) and 3-(trifluoromethyl)phenyl acetonitrile (1 g, 4.97 mmol) were dissolved in DMF (4 ml). Then piperidine (0.93 g, 10.94 mmol) followed by acetic acid (0.7 ml, 9.95 mmol) were added to the mixture. The reaction solution was refluxed for 24 hours under inert atmosphere. The reaction was monitored using TLC. After evaporation of solvent, the crude product was purified by silica gel column chromatography with ethyl acetate:hexane (1:5,v/v) as eluent. Further the product obtained was recrystallised from hexane to obtain white solid with yield 65% (1.05 g).

Molecular weight: 367.97 g/mol.

<sup>1</sup>H NMR (400 MHz, DMSO) δ 8.33 (s, J = 9.6 Hz, 1H), 8.06 (s, 1H), 8.00 (d, J = 7.8 Hz, 1H), 7.85 – 7.75 (m, 2H), 7.71 (t, J = 7.8 Hz, 1H), 7.43 (d, J = 8.8 Hz, 1H), 3.32 (s, 1H). <sup>13</sup>C NMR (101 MHz, DMSO) δ 152.41, 140.55, 135.58, 134.63, 132.79, 131.02, 129.70, 126.69, 121.43, 118.51, 116.41.

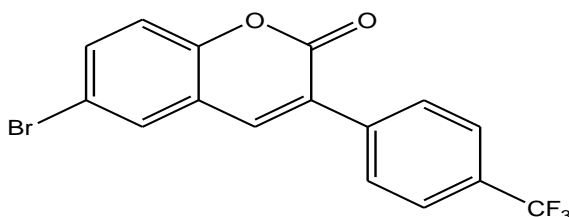


**NS-5**

*6-Bromo-3-(4-(trifluoromethyl)phenyl)-2H-chromen-2-one (NS-8).*

Into a schlenk flask, 5-bromosalicylaldehyde (1 g, 4.97 mmol) and 4-(trifluoromethyl)phenyl acetonitrile (1 g, 4.97 mmol) were added alongwith DMF (5 ml) and was continously stirred. To the dissolution, piperidine (0.93 g, 10.94 mmol) and glacial acetic acid (0.7 ml, 9.95 mmol) was dropped slowly. The reaction was kept for over 24 hours at 80 °C under inert atmosphere. The product obtained were filtered and washed with methanol to give light yellow crystals. (Yield = 45%, 0.82 g). Molecular weight: 369.13 g/mol.

$^1\text{H}$  NMR (400 MHz,  $\text{CDCl}_3$ )  $\delta$  7.87 – 7.78 (m, 3H), 7.75 (d,  $J$  = 7.5 Hz, 2H), 7.69 (dd,  $J$  = 8.8, 2.0 Hz, 1H), 2.20 (s, 1H), 2.08 (d,  $J$  = 4.4 Hz, 1H).  $^{13}\text{C}$  NMR (101 MHz,  $\text{CDCl}_3$ )  $\delta$  159.67, 152.68, 139.54, 134.94, 130.53, 129.11, 128.34, 125.70, 125.67, 120.97, 118.50, 117.45.

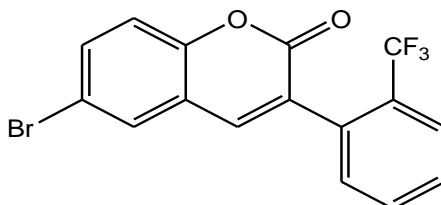


NS-8

*6-Bromo-3-(2-(trifluoromethyl)phenyl)-2H-chromen-2-one (NS-9).*

This compound was prepared with 2-(trifluoromethyl)phenyl acetonitrile following the same procedure as used for synthesis of NS-8. After recrystallization it gave yellow crystals with yield 68% (1.24 g). Molecular weight: 367.97 g/mol.

$^1\text{H}$  NMR (400 MHz,  $\text{CDCl}_3$ )  $\delta$  7.42 (d,  $J$  = 7.8 Hz, 2H), 7.04 (d,  $J$  = 7.6 Hz, 1H), 6.95 – 6.85 (m, 2H), 2.74 – 2.39 (m, 1H), 1.65 (s, 1H), 1.37 (s,  $J$  = 46.7 Hz, 1H).  $^{13}\text{C}$  NMR (101 MHz,  $\text{CDCl}_3$ )  $\delta$  159.84, 152.89, 140.66, 134.84, 132.85, 131.95, 131.74, 130.51, 129.26, 128.34, 126.74, 126.69, 123.51, 122.64, 120.45, 118.64, 117.33.

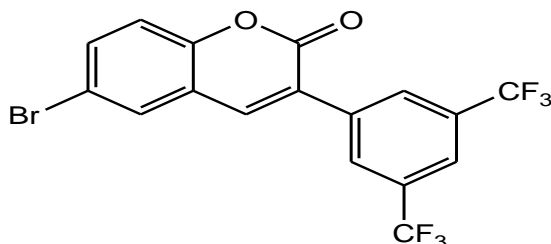


NS-9

*3-(3,5-Bis(trifluoromethyl)phenyl)-6-bromo-2H-chromen-2-one (NS-10).*

2-(3,5-Bis(trifluoromethyl)phenyl) acetonitrile (1.26 g, 4.97 mmol) and 5-bromosalicylaldehyde (1 g, 4.97 mmol) were dissolved in DMF (5 ml) in a Schlenk flask. Under inert conditions, piperidine (0.93 g, 10.94 mmol) and acetic acid (0.6 g, 9.95 mmol) were added to the reaction mixture. It was kept for about 24 hours at 80°C. After reaction completion (monitored by TLC), the solvent was evaporated. The product was then washed with methanol. Further, filtration resulted light brown solid with yield 61% (1.04 g). Molecular weight: 435.95 g/mol.

$^1\text{H}$  NMR (400 MHz,  $\text{CDCl}_3$ )  $\delta$  8.15 (s, 1H), 7.88 (d,  $J = 31.5$  Hz, 2H), 7.77 – 7.56 (m, 1H), 3.76 (d,  $J = 28.8$  Hz, 1H), 1.83 (s, 1H), 1.53 (s, 1H).  $^{13}\text{C}$  NMR (101 MHz,  $\text{CDCl}_3$ )  $\delta$  159.27, 158.26, 152.79, 152.73, 140.23, 136.30, 135.50, 132.36, 132.02, 130.72, 128.90, 126.76, 122.98, 120.61, 118.60, 117.68.



**NS-10**

### 3.3.2 General procedure for the synthesis of target compounds

A Schlenk flask was charged with 1 equivalent of previously synthesized intermediate compounds **N.S-5**, **N.S-8**, **N.S-9**, **N.S-10**, 1 equivalent of 10H-phenoxazine and 2.5 equivalent of sodium *tert*-butoxide under inert atmosphere for about 15 minutes. Toluene was then added and nitrogen was bubbled through the mixture for an hour. Thereafter, palladium (II) acetate and tri-*tert*-butyl phosphine (in 1.0 M toluene) were added. The resultant mixture was stirred for 24 hours at reflux temperature. After the reaction ended (checked by TLC), the precipitate obtained was filtered, washed with brine, dried over anhydrous  $\text{Na}_2\text{SO}_4$ . The resultant product was then purified by column chromatography on silica gel with eluent THF: hexane (1:15) to afford the target molecules **NS-5a**, **NS-8a**, **NS-9a**, **NS-10a** [39].

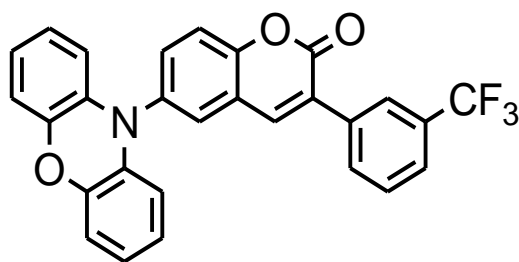
*3-(3-(Trifluoromethyl) phenyl)-6-(10H-phenoxazin-10-yl)-2H-chromen-2-one (NS-5a)*.

**N.S-5a** was prepared from **N.S-5** (0.5 g, 1.358 mmol), 10H-phenoxazine (0.25 g, 1.358 mmol), sodium *tert*-butoxide (0.326 g, 3.395 mmol), palladium (II) acetate (0.0152 g, 0.0679 mmol), tri-*tert*-butyl phosphine (0.022 g, 0.108 mmol) and toluene (10 ml) using the general procedure described above. Pale yellow crystals were obtained with 90% yield (0.57 g). Molecular weight: 471.11g/mol.

$^1\text{H}$  NMR (400 MHz,  $\text{CDCl}_3$ )  $\delta$  7.95 (d,  $J = 11.4$  Hz, 2H), 7.87 (s, 1H), 7.70 (d,  $J = 7.8$  Hz, 1H), 7.65 – 7.54 (m, 4H), 6.71 (dt,  $J = 15.0, 7.5$  Hz, 4H), 6.62 (t,  $J = 7.6$  Hz, 2H), 5.92 (d,  $J = 7.8$  Hz, 2H).

$^{13}\text{C}$  NMR (101 MHz,  $\text{CDCl}_3$ )  $\delta$  158.84, 152.20, 143.06, 138.83, 134.73, 134.13, 133.96, 133.12, 131.10, 129.83, 128.25, 126.82, 124.49, 122.46, 121.06, 120.70, 118.80, 114.91, 112.27.

IR (in KBr)  $\nu$  3068, 2962, 1725, 1625, 1590, 1484, 1328, 1267, 1117, 805, 744  $\text{cm}^{-1}$ ; MS  $m/z$  [ $\text{M}^+$ ]: 471.28.



**NS-5a**

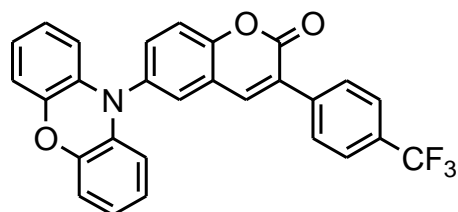
*3-(4-(Trifluoromethyl)-phenyl)-6-((-10H-phenoxazin-10-yl))-2H-chromen-2-one (NS-8a).*

**NS-8a** was prepared from **NS-8** (0.5 g, 1.358 mmol), 10*H*-phenoxazine (0.249 g, 1.358 mmol), sodium *tert*-butoxide (0.326 g, 3.395 mmol), palladium (II) acetate (0.0152 g, 0.067 mmol), tri-*tert*-butyl phosphine (0.022 g, 0.108 mmol) in toluene (10 ml) following the general procedure outlined above. Yellow crystals with yield 69% (0.44 g) was obtained. Molecular weight: 471.11 g/mol.

$^1\text{H}$  NMR (400 MHz,  $\text{CDCl}_3$ )  $\delta$  7.95 – 7.80 (m, 3H), 7.73 (d,  $J = 8.2$  Hz, 2H), 7.66 – 7.52 (m, 3H), 6.71 (dt,  $J = 15.0, 7.7$  Hz, 4H), 6.62 (dd,  $J = 11.0, 4.1$  Hz, 2H), 5.92 (d,  $J = 7.8$  Hz, 2H).

$^{13}\text{C}$  NMR (101 MHz,  $\text{CDCl}_3$ )  $\delta$  159.80, 153.23, 144.05, 140.01, 137.84, 135.72, 135.04, 134.10, 131.41, 130.85, 129.10, 127.85, 125.71, 125.67, 123.45, 122.07, 121.69, 119.79, 115.92, 113.25.

IR (in KBr)  $\nu$  3067, 1733, 1682, 1575, 1486, 1326, 1273, 1114, 946, 852, 745  $\text{cm}^{-1}$ ; MS  $m/z$  [ $\text{M}^+$ ]: 471.12.



**NS-8a**

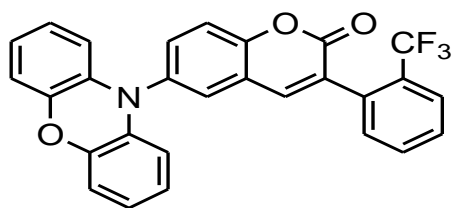
*3-(2-(Trifluoromethyl)-phenyl)-6-(10H-phenoxazin-10-yl)-2H-chromen-2-one (NS-9a).*

**NS-9a** was also prepared using the general procedure from **NS-9** (0.5 g, 1.358 mmol), 10*H*-phenoxazine (0.249 g, 1.358 mmol), sodium *tert*-butoxide (0.326 g, 3.395 mmol), palladium (II) acetate (0.0152 g, 0.0679 mmol), tri-*tert*-butyl phosphine (0.022 g, 0.1086 mmol) in toluene (8 ml) to afford yellowish crystals of yield 83% (0.53 g). Molecular weight: 471.11 g/mol.

$^1\text{H}$  NMR (400 MHz,  $\text{CDCl}_3$ )  $\delta$  7.83 (d,  $J = 17.3$  Hz, 1H), 7.79 (s, 1H), 7.70 – 7.51 (m, 5H), 7.43 (t,  $J = 9.1$  Hz, 1H), 6.81 – 6.51 (m, 5H), 5.94 (d,  $J = 7.8$  Hz, 2H).

$^{13}\text{C}$  NMR (101 MHz,  $\text{CDCl}_3$ )  $\delta$  153.45, 144.04, 141.04, 135.62, 134.98, 134.12, 132.01, 131.76, 130.76, 129.29, 129.16, 128.35, 128.00, 126.78, 125.43, 123.47, 122.01, 121.17, 119.95, 115.86, 113.32

IR (in KBr)  $\nu$  3068, 2612, 2471, 1729, 1629, 1574, 1489, 1317, 1275, 1118, 952, 750  $\text{cm}^{-1}$ ; MS  $m/z$   $[M^+]$ : 471.42.



**NS-9a**

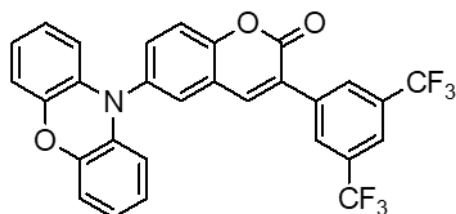
*3-(3,5-Bis(trifluoromethyl)-phenyl)-6-(10H-phenoxazin-10-yl)-2H-chromen-2-one (NS-10a).*

**NS-10a** was obtained by the general procedure described above from **NS-10** (0.5 g, 1.146 mmol), 10H-phenoxazine (0.21 g, 1.014 mmol), sodium *tert*-butoxide (0.275 g, 2.865 mmol), palladium (II) acetate (0.013 g, 0.057 mmol), tri-*tert*-butyl phosphine (0.019 g, 0.092 mmol) in toluene (10 ml) to get a yield of 62% (0.37 g) orangish solids. Molecular weight: 539.1 g/mol.

$^1\text{H}$  NMR (400 MHz,  $\text{CDCl}_3$ )  $\delta$  8.20 (s, 2H), 7.95 (s, 2H), 7.71 – 7.54 (m, 3H), 6.71 (dt,  $J = 15.1, 7.7$  Hz, 4H), 6.62 (t,  $J = 7.5$  Hz, 2H), 5.91 (d,  $J = 7.9$  Hz, 2H).

$^{13}\text{C}$  NMR (101 MHz,  $\text{CDCl}_3$ )  $\delta$  159.43, 153.33, 144.04, 140.71, 136.34, 136.01, 135.65, 134.01, 132.37, 132.04, 131.13, 128.86, 126.30, 123.45, 122.97, 122.14, 121.32, 119.94, 115.95, 113.24.

IR (in KBr)  $\nu$  3061, 2613, 2074, 1839, 1723, 1627, 1574, 1488, 1278, 1180, 1118, 899, 740  $\text{cm}^{-1}$ ; MS  $m/z$   $[M^+]$ : 539.22.



**NS-10a**

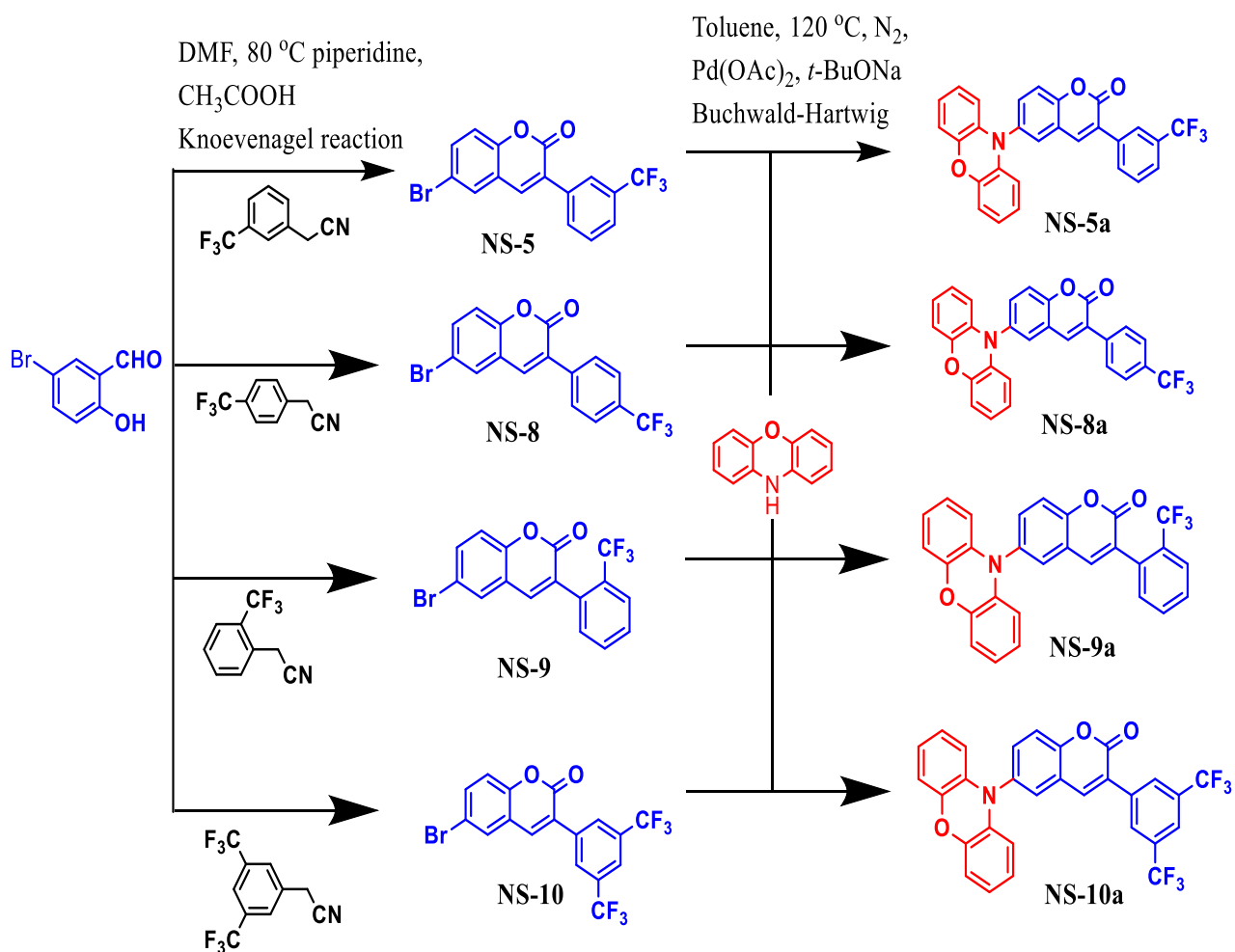
The progress of all the reactions were observed and checked by thin-layer chromatography (TLC) using aluminium sheets of silica gel.

### 3.4. Results and Discussion

#### 3.4.1. Design and synthesis

In this study, the framework for the desired compounds were based on a donor-acceptor (D-A) model, with coumarin part as acceptor and phenoxazine unit as donor. The design strategy of phenoxazine integrated coumarin compound was to mould a molecule with good steric hinderance and rigidity.

Coumarins make a promising set of organic materials in optoelectronics for its fully-fledged optical properties, stability and simpler preparation methods. Besides, substitutions in the coumarin skeleton has considerable impact on its emission wavelength [6]. Alteration of the electron-withdrawing nature of the substituent at 3-position notably upgrades the fluorecence characteristics [5]. Hence the proposed coumarin moiety was substituted at 3-position with phenyl group having trifluoromethyl moiety at different positions. The structure of phenoxazine consists of a six-membered ring with two heteroatoms which generates steric repulsion towards substituents. Consequently, the HOMO-LUMO separation required to instigate charge transfer transition is attained. In addition to that the oxygen atom on phenoxazine moiety deepens the HOMO level [8]. All these traits contributed to the choice of phenoxazine as donor unit in the target compound. In the view point of long wavelength organic emitter, the coumarin bound with phenoxazine moiety was constructed.



Scheme.1 Synthetic pathway to target compounds NS-5a, NS-8a, NS-9a, NS-10a



The synthetic routes and the chemical structures of the synthesized materials are outlined in the Scheme 1. The synthesis involved two-step procedure, consisting of Knoevenagel condensation and Buchwald-Hartwig amination. In the condensation reaction, the commercially available 5-bromosalicylaldehyde was treated with the required trifluoromethyl phenyl acetonitrile in the presence of acetic acid and piperidine to give the corresponding coumarin intermediate [38]. The electron-withdrawing group substituted phenyl acetonitriles was subsequently coupled with phenoxazine via palladium-catalyzed Buchwald-Hartwig reaction to form the corresponding products [39]. The synthesized compounds were further purified by silica gel column chromatography.

The chemical structures of the synthesized final materials were identified by mass spectrometry, IR and NMR spectroscopies. The data obtained was in good agreement with the proposed structures. The compounds **NS-8a** and **NS-10a** were found to be soluble in most of the solvents like acetone, dichloromethane chloroform etc. The  $^1\text{H}$  spectrum exhibited peaks typical of coumarin derivatives. The doublet at 7.95 ppm could be assigned to aromatic protons near the fluorocarbons. The increased chemical shift could be attributed to the electronegativity of fluorine atoms. The singlet at 7.87 ppm could be assigned to the proton (4H) of the  $\alpha$ -pyrone structure of the coumarin ring. [6]. The  $^{13}\text{C}$  NMR spectra of the final compounds, **NS-5a**, **NS-8a**, **NS-9a** and **NS-10a** showed the presence of a downfield signal at 159.7 ppm, which could be attributed to carbonyl carbon of the coumarin ring.

The IR spectra of the products **NS-5a**, **NS-8a**, **NS-9a**, **NS-10a** exhibited intense band at  $1725.08\text{ cm}^{-1}$ ,  $1732.86\text{ cm}^{-1}$ ,  $1729.06\text{ cm}^{-1}$ ,  $1722.78\text{ cm}^{-1}$  respectively, which is typical feature of coumarin compounds. This could be due to the carbonyl stretching of lactone ring of the coumarin moiety. Characteristic peaks due to the presence of trifluoromethyl group (C-F) in the compounds were observed in the region  $1400\text{--}1000\text{ cm}^{-1}$ . The weak to medium bands have been marked at  $2067\text{ cm}^{-1}$  to  $2960\text{ cm}^{-1}$  in the spectra of the coumarin derivatives. These are due to the aromatic C-H stretching vibrations. Typically for coumarins, strong bands are observed in the region  $1600\text{ cm}^{-1}$  to  $1660\text{ cm}^{-1}$  of IR spectra. In case of the synthesized materials strong bands were recorded from  $1575\text{ cm}^{-1}$  to  $1629\text{ cm}^{-1}$ , which could be ascribed to C=C skeletal vibrations. Bands for C-O-C could be observed around  $1118\text{ cm}^{-1}$  in the spectra. A number of medium to weak bands were observed in the range  $646\text{ cm}^{-1}$  to  $950\text{ cm}^{-1}$  which could be assigned to C-H bending vibrations [40,41]. The absorbance peaks found in the spectra near  $3060\text{ cm}^{-1}$  could be related to  $\text{sp}^3/\text{sp}^2$  CH stretches of the compounds.

In the mass spectra of studied coumarin derivatives (**NS-5a**, **NS-8a**, **NS-9a** **NS-10a**), the presence of molecular ion peaks at  $m/z = 471.28\text{ [M}^+]$  for NS 5a,  $471.12\text{ [M}^+]$  for NS 8a,  $471.42\text{ [M}^+]$  for **NS-9a** and  $539.22\text{ [M}^+]$  for **NS-10a** confirmed the proposed structures.

### X-ray single crystal analysis

Single crystal of coumarin derivative **NS-8a** was obtained employing slow evaporation from solvent mixture, DCM/acetone. The crystal structure of **NS-8a** crystallizes in a triclinic space group P-1. The structure analysis demonstrated that both phenoxazine and coumarin moieties had  $\pi$ -conjugated planar structure [42]. The highly twisted structure with dihedral angle between the acceptor coumarin moiety and phenoxazine moiety was noticeable. This could further facilitate efficient charge transfer ability. The structure obtained was in agreement with the proposed structure of the coumarin derivative, **NS-8a**.

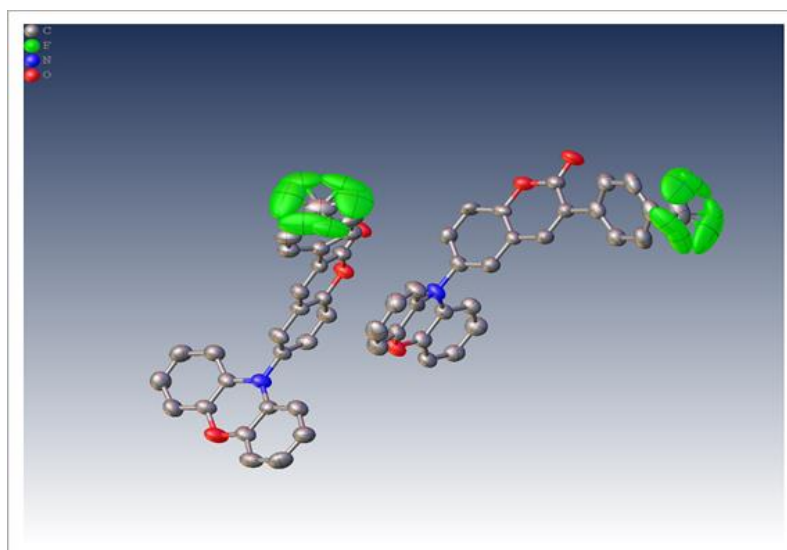


**Fig. 11.** Single crystal structure of the compound **NS-8a**

### 3.4.2. Thermal properties

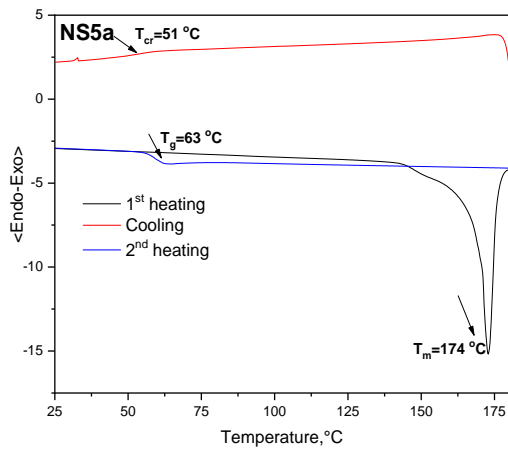
Thermal properties of the compounds **NS-5a**, **NS-8a**, **NS-9a**, **NS-10a** were investigated by thermogravimetric analysis (TGA) and differential scanning calorimetry (DSC) under nitrogen atmosphere. The decomposition temperature (5% weight loss) and the glass transition temperature are significant factors that reveal the thermal and morphological stability of organic materials [43]. The thermal stability of the compounds are estimated using TGA measurement. The values of the melting points ( $T_m$ ), glass transition temperature ( $T_g$ ), 5% weight loss temperatures ( $T_d$ ) and crystallisation temperature ( $T_{cr}$ ) are summarised in Table 3.

Thermal stability of a compound could be described as the temperature upto which 95 % of the constituents of the compound will remain stable under heating [5]. Thus the stability of the coumarin derivatives were examined using TGA.

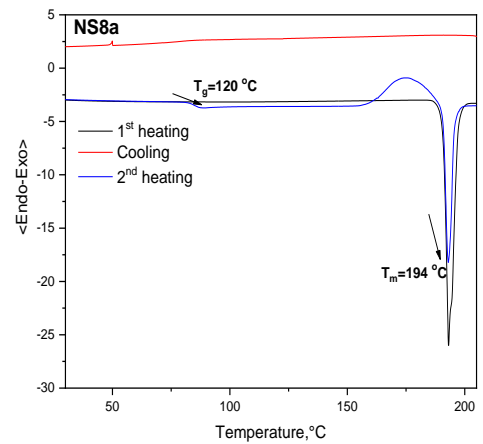
**Table 3.** Thermal characteristics of the coumarin derivatives, **NS-5a**, **NS-8a**, **NS-9a**, **NS-10a**

Compound	$T_m^a$ , °C	$T_g^b$ , °C	$T_d^c$ 5%, °C	$T_{cr}^d$ , °C
<b>NS-5a</b>	174	63	345	51
<b>NS-8a</b>	194	120	356	-
<b>NS-9a</b>	275	83	310	71
<b>NS-10a</b>	264	80	328	-

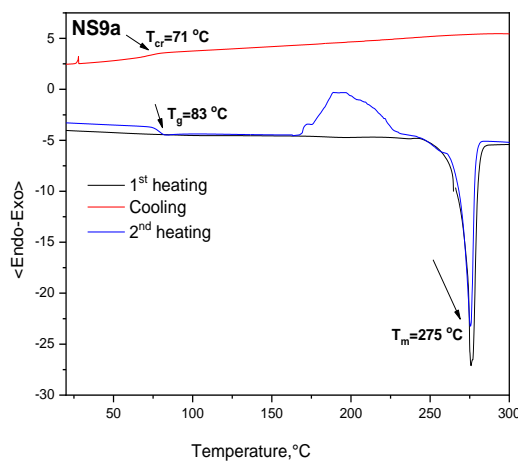
- Melting point.
- Glass transition from DSC curves observed at the first heating scan of DSC measurement.
- 5% weight loss destruction temperature obtained from TGA curves.
- Crystallisation temperature.



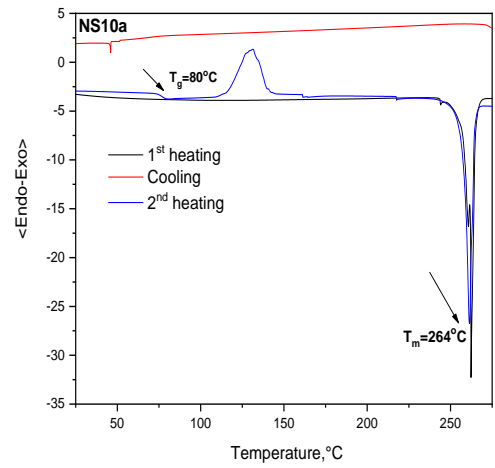
**NS-5a**



**NS-8a**

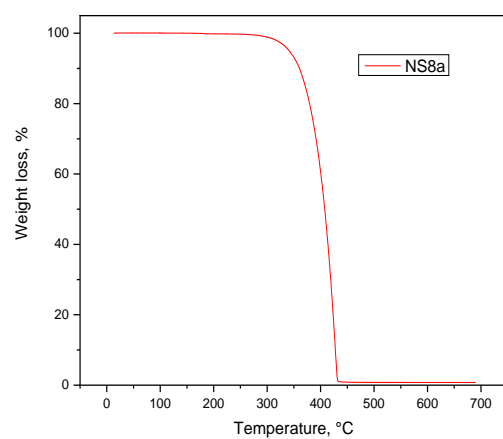
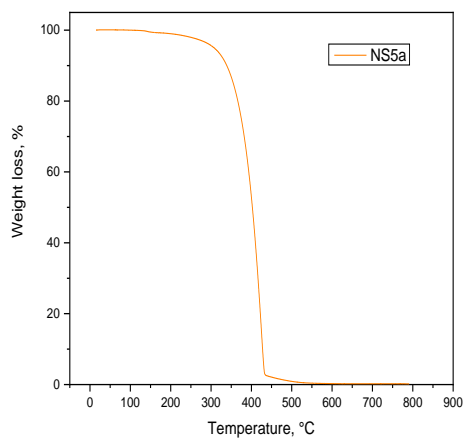


**NS-9a**



**NS-10a**

**Fig. 12. DSC thermograms of NS-5a, NS-8a, NS-9a and NS-10a**



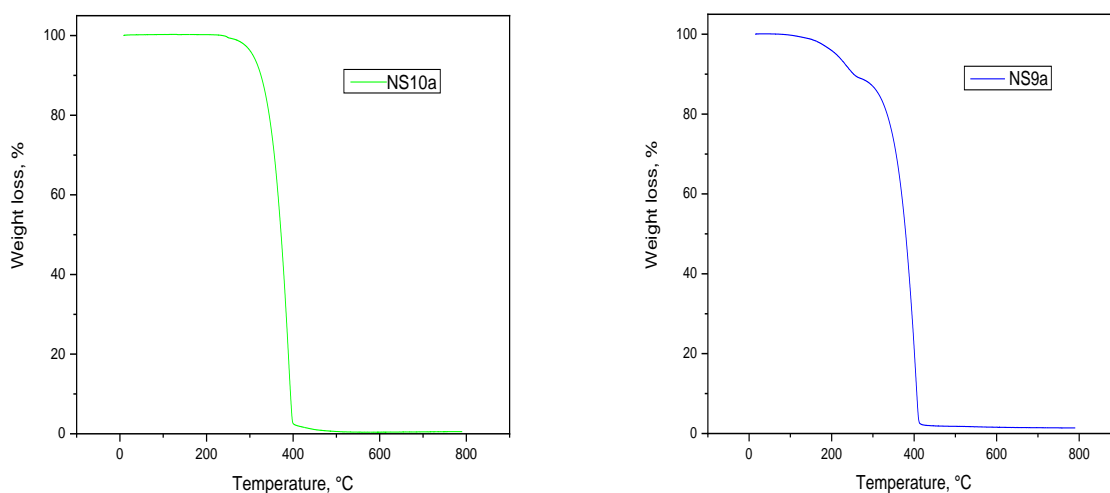


**Fig. 13.** TGA curves of **NS-5a**, **NS-8a**, **NS-9a** and **NS-10a**

The DSC thermograms and TGA curves of the final compounds, **NS-5a**, **NS-8a**, **NS-9a** and **NS-10a** are given in Figure 12 and Figure 13 respectively. Typically, molecular weight and thermal traits of a compound are directly related to each other. Hence, high melting point, glass transition and thermal decomposition temperatures could be found in high molecular weight compounds [43]. All the coumarin derivatives substituted with trifluorotoluene (**NS-5a**, **NS-8a** and **NS-9a**) except **NS-10a**, have the same molecular weight. Therefore, similarity in thermal behaviour is anticipated for these materials. All the compounds exhibited similar 5% weight loss temperatures ( $T_d$ ) that varies from 310 °C to 356 °C, measured by TGA (Figure 12). In DSC measurement, during the first heating scan a sharp endotherm was observed which gives melting point temperature ( $T_m$ ). The melting points were in the range from 164 °C to 274 °C. In case of compounds **NS-5a** and **NS-9a**, exothermic crystallisation peaks were observed during the cooling scans, whereas for compounds **NS-8a** and **NS-10a** crystallisation temperature was not observed.

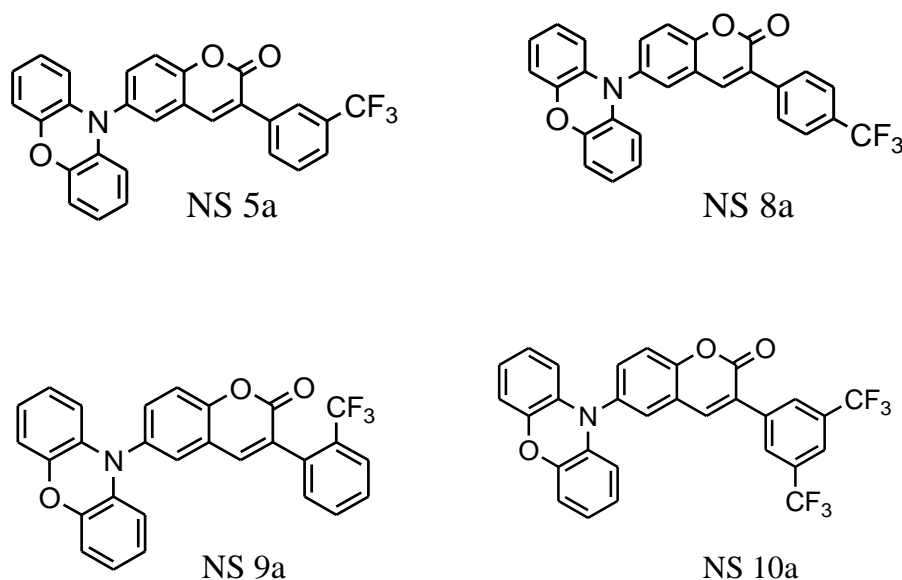
The crystalline sample of **NS-5a** melted at 174 °C in the first heating scan, on further cooling the melt crystals were formed at 51 °C. Upon second heating, glass transition was recorded at 63 °C. The crystalline sample **NS-8a** under first heating scan melted at 194 °C and under cooling scan, crystallisation signal was not observed. Glass transition was observed on second heating of the sample at 120 °C and a second melting was recorded at the same temperature as the first melting (194 °C). The solid sample **NS-9a** demonstrated melting at 275 °C in the first heating scan and crystallisation was noted when cooled to 71 °C. But upon second heating, glassy state was acquired at 83 °C and second melting at 276 °C. As for the compound **NS-10a**, melting point was observed at 264 °C during first heating with no crystallisation signals observed on cooling. However glass transitions was found at 80 °C and second melting was exhibited at the same temperature as first melting. The melting temperatures of **NS-9a** and **NS-10a** are comparatively higher than that of **NS-5a** and **NS-8a**. Highest glass transition temperature was exhibited in **NS-8a** among all the synthesized materials. The variation of trifluoromethyl group at different positions on the phenyl moiety of coumarin acceptor contributes to the thermal stability of the four coumarin based compounds. Due to the strong electronegative character of trifluoromethyl group, strong push and pull phenomena occurs between

free radicals of fluorine. This contributed to the thermal behaviour of the final products, **NS-5a**, **NS-8a**, **NS-9a** and **NS-10a**.

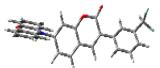
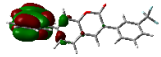
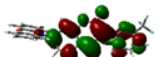
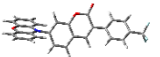
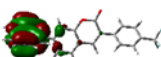
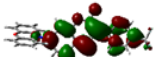
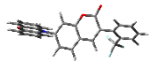
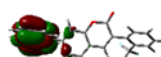
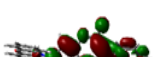
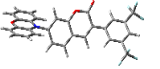
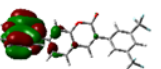
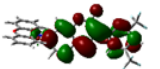
In general, the organic materials applied in OLEDs have comparatively lower melting point temperatures due to weaker Van der Waals interaction forces. This provides flexibility to OLED devices, facilitating efficient operations [47]. The investigations on the thermal behaviour of the derived compounds clearly depicted that they have good thermal stability and adequate characteristics for vapor deposition in OLED fabrication.

### 3.4.3. Theoretical studies

In an effort to better understand the structure-property relationship of the compounds synthesized, density functional theory (DFT) was done. Theoretical calculations based on DFT method was conducted on the final materials in order to have a perspective of their HOMO/LUMO distribution. The optimized structures of the compounds **NS-5a**, **NS-8a**, **NS-9a**, **NS-10a** were acquired by DFT calculations at the B3LYP/6-31G(d,p) level (Figure 15). The optimized structures of the compounds **NS-5a**, **NS-8a**, **NS-9a** and **NS-10a** have twisted structures with dihedral angles between the electron-donating (phenoxazinyl) and electron-accepting (coumarin) moieties ranging from 70° to 79°. The twisted structures of compounds **NS-5a**, **NS-8a**, **NS-9a**, **NS-10a** lead to a spatially separated frontier orbital distributions highest occupied molecular orbitals (HOMOs) being mainly localised on the donor (phenoxazinyl) moieties and the lowest unoccupied molecular orbitals (LUMOs) centered on the acceptor (coumarin) moieties. The HOMO energy levels of the compounds **NS-5a**, **NS-8a**, **NS-9a**, **NS-10a** were calculated to be -4.90 eV, -4.92 eV, -4.83 eV and -4.99 eV while the LUMO levels were -2.43 eV, -2.47 eV, -2.25 eV and -2.66 eV, respectively.



**Fig. 14.** Chemical structures of the target compounds, **NS-5a**, **NS-8a**, **NS-9a**, **NS-10a**

Compound	Optimized geometries	HOMO (eV)	LUMO (eV)
NS-5a		 - 4.90	 -2.43
NS-8a		 -4.92	 -2.47
NS-9a		 -4.83	 -2.25
NS-10a		 -4.99	 -2.66

**Fig. 15.** Theoretically calculated HOMO and LUMO levels distributions and optimized geometries of NS-5a, NS-8a, NS-9a, NS-10a DFT calculations were performed at the B3LYP/6-31G (d,p)

Energy levels form a cardinal part in the characterization of electroactive materials employed in OLEDs. The color of the light emitted depends on the energy band gap of the emissive layer utilized [47]. The values obtained from theoretical calculations were comparable with those obtained from previously reported coumarin derivatives.

#### 3.4.4. Electrochemical properties

Cyclic Voltammetry (CV) is an accurate technique to enlighten the electron transfer process in an organic molecule correlating potential (V) and current [47]. The stability of synthesized materials when tested electrochemically has great influence on its applicability in optoelectronic devices. Different redox processes occur when current is introduced to solution of target materials. In cases where reduction of molecule to its initial state happens as a result of oxidation of molecule to radical cation, reversible oxidation could be predicted. Irreversible process is said to occur, if there is a decline in current or an additional wave is found during multiple scans. CV aids to find the energy required for removal of one electron from a molecule [3].

Cyclic voltammetry was employed to investigate electrochemical properties of compounds NS-5a, NS-8a, NS-9a and NS-10a. They showed single oxidation peaks, which can be assigned to the formation of radical cations of the electron-donating phenoxazinyl moiety (Figure 16). The

compounds showed a close spread of oxidation potentials versus the ferrocenium/ferrocene (Fc/Fc<sup>+</sup>) (0.35 V) redox couple. Ionization potential (IP<sub>CV</sub>) values were calculated by the formula  $IP_{CV} = |-(1.4 \times 10^{-1} e^{-E_{onset}^{ox} vs Fc/V}) - 4.6| eV$ . The data are summarised in Table 4. IP<sub>CV</sub> values were found to be comparable (5.09 eV). Electron affinities (EA<sub>CV</sub>) estimated using the optical band gaps (E<sub>g</sub>) and IP<sub>CV</sub> values to be ranging from 3.35 to 3.40 eV. The ionization potential could be correlated to HOMO energy level and the electron affinity to LUMO energy level. The energy difference between the HOMO and LUMO energy level corresponds to the E<sub>g</sub> [44]. In instances when no reduction wave is detected, LUMO levels are reckoned from the HOMO level and the optical band gap [45].

The CV analysis alongwith UV-Vis spectroscopy provide details of electron affinity, ionization potential and band gap energies, which can be applied for building new stable and efficient organic devices. In particular, for OLED applicability, information on energy level is indispensable. Based on this knowledge, appropriate host required for the emitter synthesized could be decided effectively. In addition to that other active layers recommended for desired functioning of OLED devices could also be properly selected [46]. Electrochemical measurement is a way to evaluate the applicability of materials by testing them under conditions relative to working organic electronic devices.

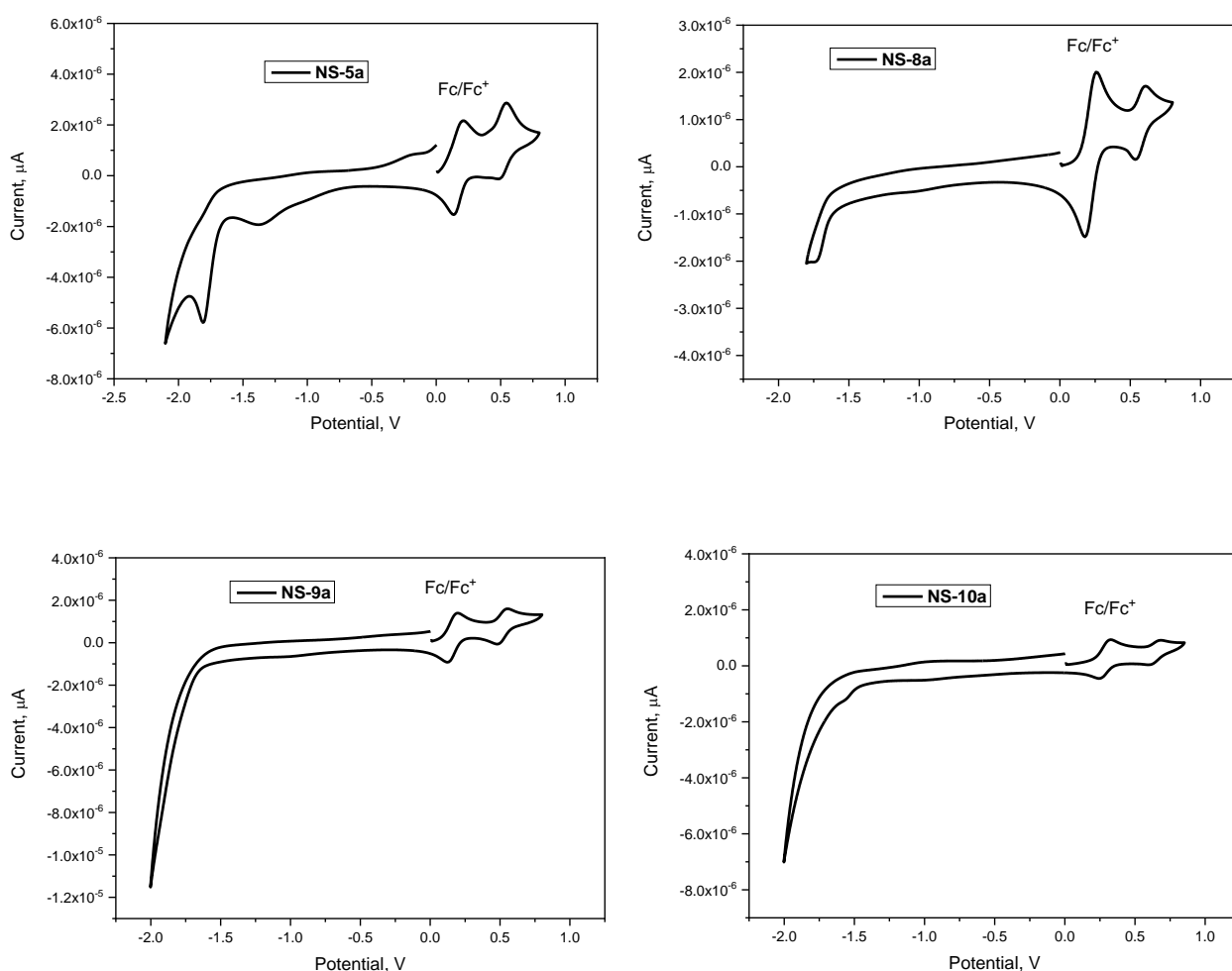


**Fig. 16.** CV curves of dilute solutions of derivatives **NS-5a**, **NS-8a**, **NS-9a**, **NS-10a** in dichloromethane (100mV/s)

**Table 4.** Oxidation potential, ionization potential electron affinity of **NS-5a**, **NS-8a**, **NS-9a** and **NS-10a**

Derivative	$E_{\text{onset}}^{\text{ox}}$ vs Fc [V]	$IP_{\text{CV}}^{\text{a}}$ [eV]	$EA_{\text{CV}}^{\text{b}}$ [eV]	$E_{\text{g}}^{\text{opt}}$ [eV]
NS 5a	0.35	5.09	1.74	3.35
NS 8a	0.35	5.09	1.74	3.35
NS 9a	0.35	5.09	1.69	3.40
NS 10a	0.35	5.09	1.69	3.40

$$IP_{\text{CV}} = |-(1.4 \times 10^{-1} e^{-E_{\text{onset}}^{\text{ox}} \text{ vs Fc}/V}) - 4.6| \text{ eV.}$$

[a] Ionization potential values according to

$$EA_{\text{CV}} = -(|IP_{\text{CV}}| - E_{\text{g}}^{\text{opt}})$$

[b] Electron affinity value

$E_{\text{g}}^{\text{opt}} = 1240/\lambda_{\text{edge}}$ ,  $\lambda_{\text{edge}}$  is the onset wavelength of absorption spectrum of the dilute chloroform solution.

The compounds **NS-5a**, **NS-8a**, **NS-9a** and **NS-10a** have identical HOMO levels as they have the same donor, phenoxazinyl moiety. The final products have reasonable electrochemical stability for utilization in optoelectronics.

### 3.4.5. Photoelectrical properties

The incident light photon energy ( $h\nu$ ) has significant impact on photocurrent. A plot with  $I^{0.5} = f(h\nu)$  dependance was deduced. Photon energy was ascertained from the interception point on the x-axis ( $h\nu$ ) with the extrapolated linear part of the dependance [43]. Solid state ionisation potential (IP) of **NS-5a**, **NS-8a**, **NS-9a**, **NS-10a** was recorded from their solid layer by electron photoemission method. Figure 17 illustrates the photoemission spectra of the films of the researched molecules, **NS-5a**, **NS-8a**, **NS-9a** and **NS-10a**.



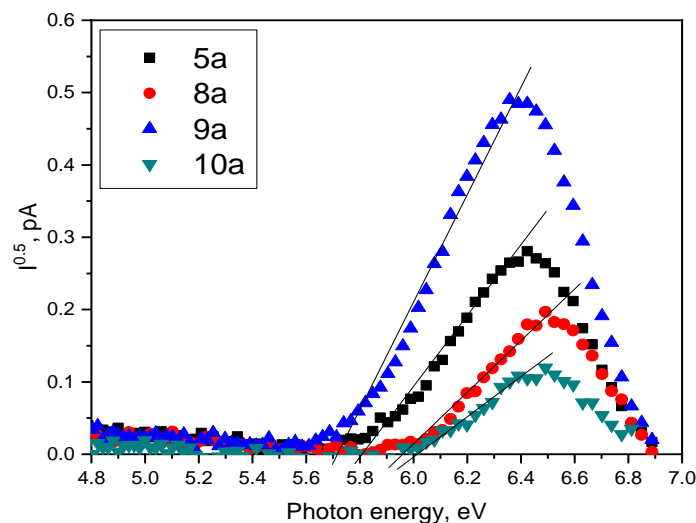


**Fig. 17.** Electron photoemission spectrum of the vacuum solid film of **NS-5a**, **NS-8a**, **NS-9a**, **NS-10a**

The IP value observed of the compounds, **NS-5a**, **NS-8a**, **NS-9a** and **NS-10a**, using photoemission method was higher than that assessed from electrochemical measurements. Such disagreements in the value of IP could be evidently due to the intermolecular interactions of molecules that can take place in the solid layers. The values of ionization potential recorded were in the range of 5.72 eV to 5.98 eV. Compound **NS-9a** demonstrated the lowest ionization potential of 5.72 eV among all the synthesized coumarin compounds.

From all the electrochemical values observed, compound synthesized with fluorocarbon substitution at ortho-position of the phenyl ring of the coumarin moiety showed the least of all. While, para-substituted (**NS-8a**) was higher than meta-substituted derivative (**NS-5a**). The derivative **NS-10a** having trifluoromethyl substitutions at 3 and 5-positions displayed the highest electrochemical values of all the synthesized materials.

The values obtained from all the electrochemical investigation of the target compounds were comparable to the reference coumarin derivatives, **PHzMCO** and **PHzBCO** [35]. The analysis by electron photoemission is significant as they give appropriate details in charge balancing in optoelectronic applications [3].

### 3.4.6. Photophysical properties

An UV-Vis spectrum gives information about the wavelength at which maximum absorption of energy by a molecule takes place and its excitation limit. Absorption and fluorescence spectra of the synthesized compounds, **NS-5a**, **NS-8a**, **NS-9a**, **NS-10a** in various solvents are illustrated in Figure 18 and Figure 19. Two intense absorption bands were detected in the absorption spectra of dilute solutions in  $\text{CHCl}_3$  and THF. The wavelengths of absorption maxima of the higher energy bands (at *ca* 300 nm) were found to be close to that of phenoxazine moiety. These characteristic bands could be ascribed to the  $\pi\text{-}\pi^*$  electronic transitions of the coumarin moiety.

The absorption profiles of all the compounds were quite similar though there was a slight difference in the spectra of compound **NS-9a**. The presence of three bands in the spectra of **NS-9a** was noted.

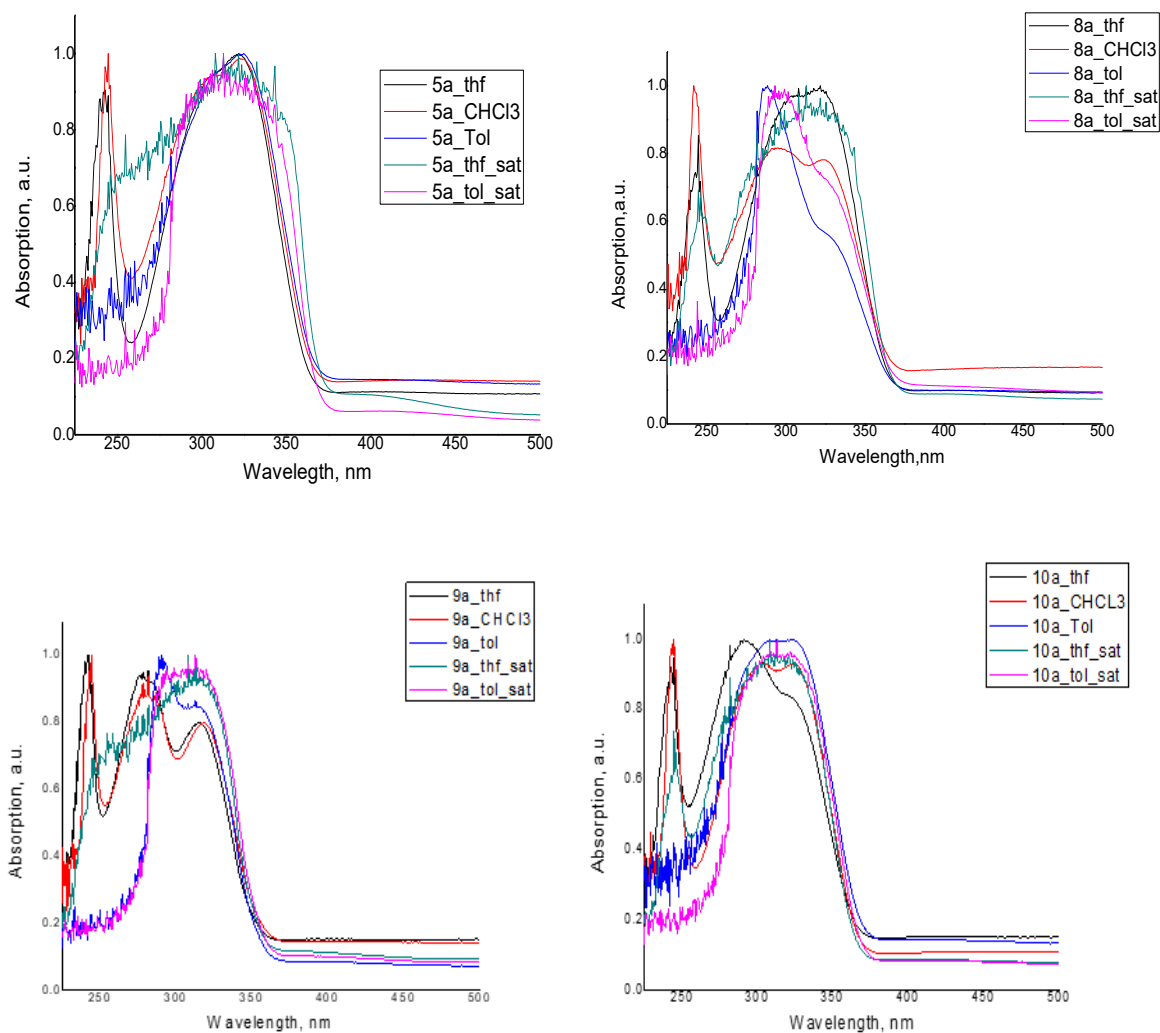


**Fig. 18.** Absorption spectra of compounds **NS-5a**, **NS-8a**, **NS-9a** **NS-10a** in solvents (THF,  $\text{CHCl}_3$ , toluene)

The coumarin-based compounds, **NS-5a**, **NS-8a**, **NS-9a** and **NS-10a** exhibit absorption maxima bands from 300 nm. The strong absorption bands at around 300 nm could be assigned to  $\pi$ - $\pi^*$  transition of phenoxazine, while the broader absorption minimas could be related to the intercharge transfer from phenoxazine moiety to coumarin moiety. From the absorption edge ( $\lambda_{\text{edge}}$ ), optical band gap ( $E_g$ ) could be evaluated. The coumarin derivative **NS-8a** red shifted the highest among the derivatives studied. This may be due to the effect of fluorocarbon substituent at the para position of the phenyl linkage of coumarin moiety. However, fluorocarbon substitutions at position 3 and 5 does not seem to have effect on the intercharge transfer effect in the molecule.

The stokes shift of the target compounds in solution was calculated and are outlined in Table 6. Stokes shift is a vital concept, denoting the spectral difference of emission to longer wavelengths compared to absorption. All the compounds in their solid films exhibited large stokes shift, denoting higher energy loss during the emission process. On the contrary, the stokes shift in solution of coumarin derivative **NS-5a** was noted to be smaller (43-70 nm in different solvents). This makes

coumarin derivative **NS-5a** to have higher fluorescence efficiency as well as a good candidate for OLED application. Larger Stokes shift values could be indicative of intramolecular energy transfers in the synthesized molecules.

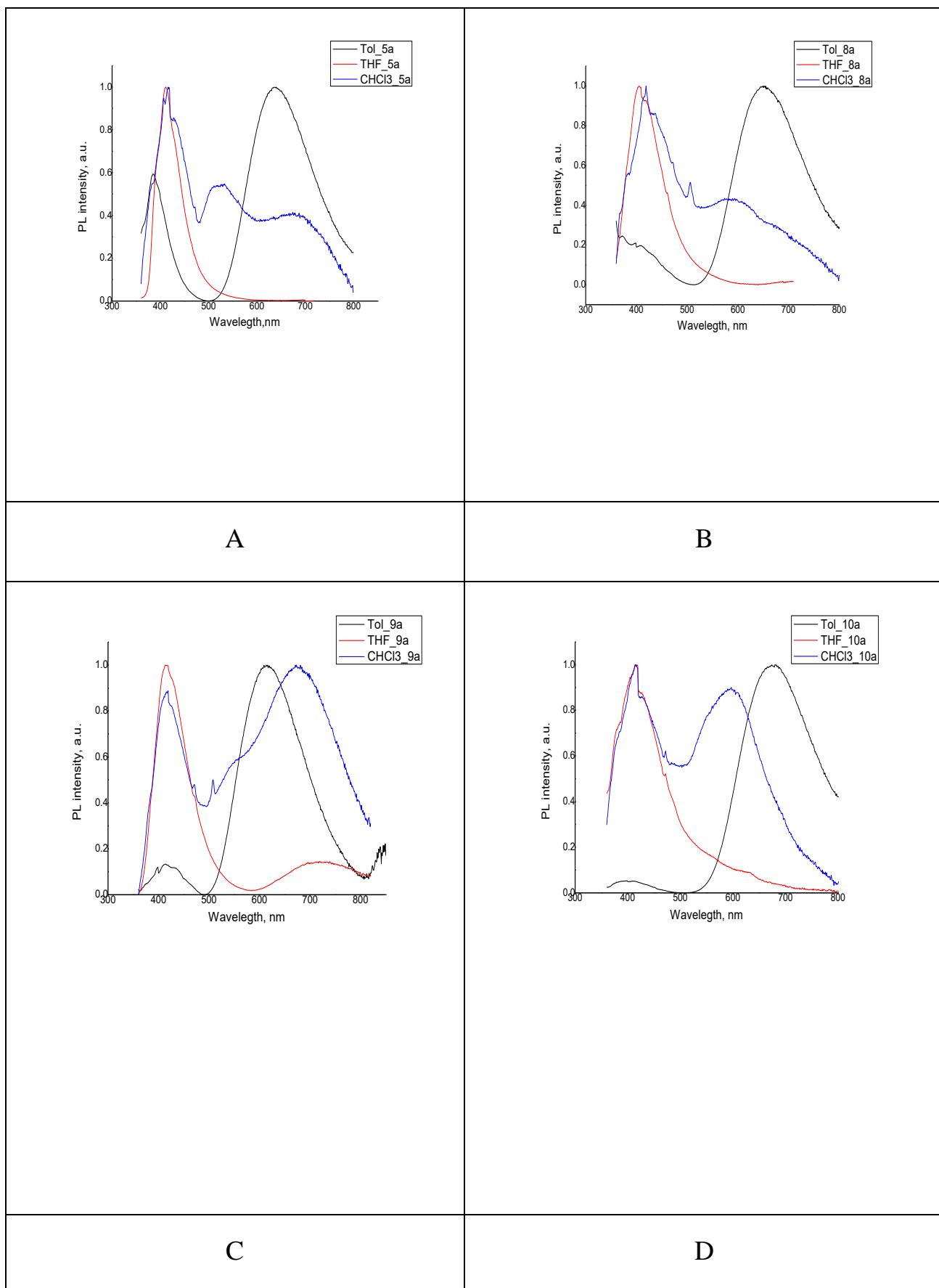


**Fig. 19.** Photoluminescence spectra of compounds **NS-5a**, **NS-8a**, **NS-9a**, **NS-10a** in different solvents (toluene, CHCl<sub>3</sub>, THF)

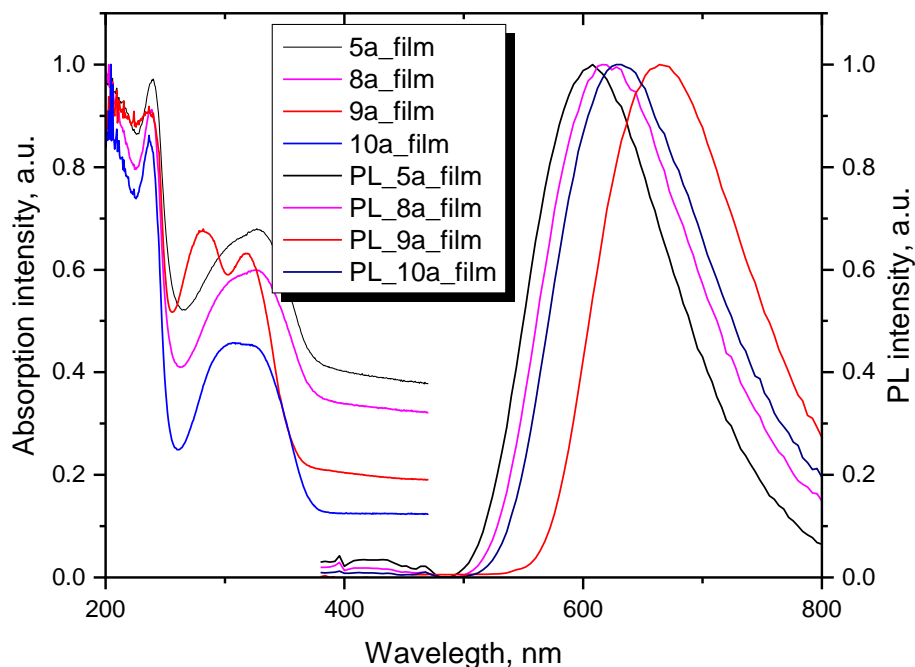


**Fig. 20.** Absorption and photoluminescence spectra of solid films of compounds **NS-5a**, **NS-8a**, **NS-9a** and **NS-10a**

**Table 5.** Photophysical characteristics of the compounds (**NS-5a**, **NS-8a**, **NS-9a** and **NS-10a**)

Compound	Solution						$\Phi_{PL}$ , %	Thin film		
	Toluene		THF		CHCl <sub>3</sub>			UV: $\lambda_{edge}$ , nm	$\lambda_{max.PL}$ , nm	$\Phi_{PL}$ , %
	UV: $\lambda_{edge}$ , nm	$\lambda_{max.PL}$ , nm	UV: $\lambda_{edge}$ , nm	$\lambda_{max.PL}$ , nm	UV: $\lambda_{edge}$ , nm	$\lambda_{max.PL}$ , nm				
<b>NS-5a</b>	322	384,635	243,322	410	243,322	410,522, 670	0.06	240,325	605	0.7
<b>NS-8a</b>	288	650	243,322	405	241,292, 324	420,595	0.05	235,325	620	0.1
<b>NS-9a</b>	290,315	415,612	242,277, 315	412	243,281, 318	412,670	0.06	235,282, 317	665	0.8
<b>NS-10a</b>	315	677	243,302, 323	415	243,302, 323	415,595	0.01	235,315	630	0.3

$\Phi_{PL}$  = Fluorescence quantum efficiency, %

**Table 6.** Comparison of the spectral properties of the researched compounds, **NS-5a**, **NS-8a**, **NS-9a**, **NS-10a**

Solvents	Compounds											
	NS-5a			NS-8a			NS-9a			NS-10a		
	$\lambda_{\text{abs}}$ nm	$\lambda_{\text{em}}$ nm	Stokes shift nm <sup>a</sup>	$\lambda_{\text{abs}}$ nm	$\lambda_{\text{em}}$ nm	Stokes shift nm <sup>a</sup>	$\lambda_{\text{abs}}$ nm	$\lambda_{\text{em}}$ nm	Stokes shift nm <sup>a</sup>	$\lambda_{\text{abs}}$ nm	$\lambda_{\text{em}}$ nm	Stokes shift nm <sup>a</sup>
Toluene	341	384	43	294	650	356	310	612	302	320	677	357
THF	332	410	78	340	405	65	340	412	72	292	415	123
CHCl <sub>3</sub>	340	410	70	348	420	72	280	610	330	338	595	257

<sup>a</sup> – Stokes shift calculated using,  $\text{stokes shift} = \lambda_{\text{max}}^{\text{em}} - \lambda_{\text{max}}^{\text{abs}}$

The fluorescence spectra of the coumarin compounds (**NS-5a**, **NS-8a**, **NS-9a**, **NS-10a**) was assessed to have resemblance to the absorption spectra. Bathochromic shifts of coumarin derivatives **NS-5a**, **NS-10a** were confirmed from the maximum intensity shifts to longer wavelengths compared to that of compounds **NS-8a** and **NS-9a**. In addition to that, fluorescence intensity maxima of derivatives (**NS-5a**, **NS-9a**) evinced bathochromic shifts when related to those of coumarin derivatives. Vibronic spectral characteristics were not present in the emission spectra of the solid film of final products (**NS-5a**, **NS-8a**, **NS-9a**, **NS-10a**) but were detected in case of the dilute solutions in toluene (less polar) and in THF (more polar). The emission intensity maxima of the solutions of these four compounds in toluene showed red shifted in comparison to those of the solutions in THF.

In order to scrutinize the solvatochromic effect on the fluorescence properties, fluorescence spectra of the compounds was measured in solvents of varying polarity (THF, chloroform, toluene). The effect of solvent polarity on the emission spectra was larger (*ca.* 250 nm) in compounds **NS-5a** and **NS-9a** compared with that perceived for compounds **NS-8a** and **NS-10a** (*ca.* 180 nm). The variations in solvation of ground state and first excited state of the light absorbing molecule results in solvatochromism [43].

Fluorescence quantum yield measures how efficient the process of emitting light from the desired molecule occurs. It could be found from the ratio of number of photons emitted to the number of

photons absorbed [43]. The fluorescence quantum yield of the film of the target compounds were not similar. The compounds **NS-5a** and **NS-9a** showed highest quantum yield of 0.7 and 0.8 among the four synthesized coumarin derivatives. But, the quantum yield of these compounds in solutions were similar. The lower yields in compounds, **NS-8a** and **NS-10a** could be the result of other mechanisms such as intersystem crossing and internal conversions during photon emission. The quantum yield of the derivative **NS-8a** was higher in solution than in film. Nevertheless, the quantum yield of the researched compounds were comparable and slightly higher with the coumarin derivatives referred in the literature. Decrease in fluorescence efficiency was found in solutions of all the compounds though increase was observed in their fluorescence efficiency of solid films. The photophysical characteristics were investigated as they correlate the molecular structure and the absorption-emission traits of the synthesized coumarin compounds. The high quantum yield of solid films of coumarin compounds **NS-5a** and **NS-9a** could make them potential for optoelectronic applications.

It has been observed that substitutions on the coumarin core with strong donating or accepting fragments, have influence on photophysical properties of coumarin derivatives. To elaborate, increase in stokes shift have been found upon substitution at position-3 [48]. Similar observations have been established with the coumarin derivatives in this study. Coumarin substituted at C-3 with phenyl having fluorocarbon fragments at two positions (**NS-10a**), were assessed to show higher stokes shift than other coumarin derivatives.

#### 4. Recommendations

##### Technological Scheme for the production of coumarin derivatives NS-5a, NS-8a, NS-9a, NS-10a

A technological scheme for the production of the coumarin derived compounds **NS-5a, NS-8a, NS-9a, NS-10a** is outlined in the scheme given below. The production sequence of the desired compounds consists mainly of two stages. The intermediates **NS-5, NS-8, NS-9, NS-10** are formed during the first stage, which in turn utilised for the second stage of production. Each stage involves purification of the products which enhances the yield of the entire process.

The intermediate coumarins **NS-5, NS-8, NS-9, NS-10** are prepared in the reactor vessel R1. The starting materials 5-bromosalicylaldehyde and 3-(trifluoromethyl)phenyl acetonitrile, 4-(trifluoromethyl)phenyl acetonitrile, 2-(trifluoromethyl)phenyl acetonitrile or 3,5-bis(trifluoromethyl)phenyl acetonitrile are added from their respective storage tanks a1 and a2 at the beginning, controlled through manual globe valves. Inert gas argon is supplied into the reactor from gas cylinder a5, to remove dissolved oxygen, thus preventing any unwanted reactions. Thereafter, the solvent DMF is supplied to dissolve the raw materials. An agitator is provided inside the reactor to evenly mix the compounds for effective synthesis. Piperidine is added slowly from its storage tank a3 and acetic acid from tank a4. The temperature is controlled and maintained around 80 °C for about 24 h. After reaction completion, the reactor is cooled to room temperature. The product solution obtained is further send to filtration tank, where the solid product is separated from the mixture. The product obtained is further purified by washing it with methanol. The purified solids are then introduced in vaccum dryer to afford dry powder product (PR1), which is stored in tank S1.

The second stage of the process starts with the product obtained from the previous reaction, PR1. The required amount calculated from the yield of the first reaction (**NS-5, NS-8, NS-9, NS-10**) is charged in the second reactor vessel R2. Thereafter, 10*H*-phenoxazine and sodium *tert*-butoxide are injected from b1 and b2, respectively. Inert gas is then added to the reactor system. Toluene is introduced and the dissolution is bubbled with nitrogen gas. This evenly dissolves and makes a uniform mixture in the reactor. The reaction mixture is then kept for an hour and the ligand, tri-*tert*-butylphosphine and palladium (II) acetate was injected to it from the storage tanks b3 and b4, respectively. The resultant mixture was refluxed for more than 24 h. After the reaction ends, it is allowed to cool. The cooled product PR2 is then sent for extraction using ethyl acetate and distilled water. The organic phase is separated out in the extraction tank E using organic solvents. The extraction solvent is separated from the product and regenerated using the evaporator F. Condenser N is used for regenerating the solvent back to be used in the extractor. The separated product is passed through a fixed bed column M for further removal of impurities. The absorption bed used in the column is made of silica gel. The product is selectively removed by the use of UV. The product stream as well as the rejected impurity streams have to undergo regeneration of the eluent. The eluents recycled are further stored in a storage sphere, from where it could be pumped when need arises in the column. The solids obtained from the product stream PR2 is then passed to a draft-tube crystallizer, where with the help of methanol, crystals of high purity are formed. The crystal is removed from the slurry in the filtration tank F2 and are later fully dried off in the dryer D2 to remove any leftover moisture. The target compounds (**NS-5a, NS-8a, NS-9a, NS-10a**) obtained are then stored in the storage container S2.

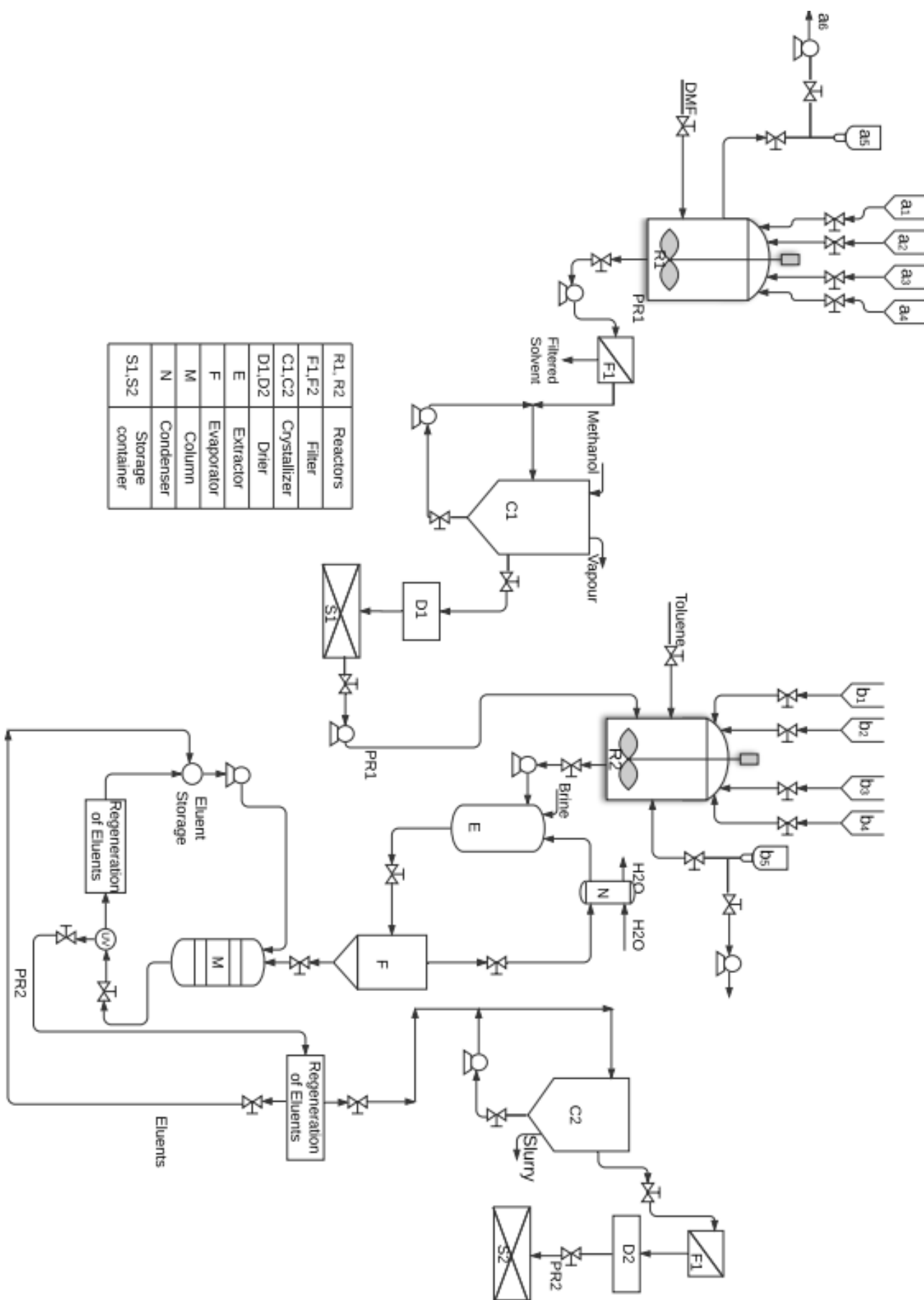


Fig. 21. Technological line for the production of coumarin derivatives NS-5a, NS-8a, NS-9a, NS-10a



## 5. Occupational safety and health


### 5.1. Characteristic of designed materials






- a) Location of the company: research laboratory for semiconductors (Room: A209), Department of Polymer and Chemical Technology, Radvilenu Plentas, Kaunas.
- b) Purpose of the company: delivering educational and other services to individuals, nurturing them to become researchers on a global level as well as contributing to the world community, innovations beneficial for daily life.
- c) Materials used: 5-bromosalicylaldehyde, 3-(trifluoromethyl)phenylacetonitrile, 4-(trifluoromethyl)phenylacetonitrile, 2-(trifluoromethyl)phenylacetonitrile, 3,5-bis(trifluoromethyl)phenyl acetonitrile, piperidine, acetic acid, 10*H*-phenoxazine, sodium *tert*-butoxide, palladium (II) acetate, tri-*tert*-butyl phosphine in 1.0 M toluene, dimethyl formamide, toluene, methanol, hexane, ethyl acetate, dichloromethane, acetone, chloroform-*d*, dimethyl sulfoxide-*d*, argon, silica gel
- d) Synthesized materials:
  - **NS-5a**: 3-(3-(trifluoromethyl)phenyl)-6-(10*H*-phenoxazin-10-yl)-2*H*-chromen-2-one.
  - **NS-8a**: 3-(4-(trifluoromethyl)phenyl)-6-(10*H*-phenoxazin-10-yl)-2*H*-chromen-2-one.
  - **NS-9a**: 3-(2-(trifluoromethyl)phenyl)-6-(10*H*-phenoxazin-10-yl)-2*H*-chromen-2-one.
  - **NS-10a**: 3-(3,5-bis(trifluoromethyl)phenyl)-6-(10*H*-phenoxazin-10-yl)-2*H*-chromen-2-one.








### 5.2. Occupational risk assessment

- a) Chemical agents

**Table 7.** Description of materials and its hazardous properties [49]

Compound	Hazard symbol	Hazard statement	Measures
3-(Trifluoromethyl)phenylacetonitrile		Flammable liquid(H226) Causes skin irritation (H315) Causes serious eye irritation (H319) May cause respiratory irritation (H335) Wear protective gloves/ protective clothing (P280) If in eyes,rinse cautiously with water.(P305+P351+P338) Keep away from heat and other ignition sources (P210) WGK Germany 3	Fire fighting measures: Suitable extinguishing media- Dry sand Do not use waterjets  First aid measures: If inhaled, provide fresh air In case of skin contact, wash off with soap and water In case of eye contact, rinse thoroughly with water for 15 minutes. General advice : consult a physician

4-(Trifluoromethyl) phenylacetonitrile		Causes skin irritation (H315) Cause serious eye irritation (H319) Harmful if swallowed, in contact with skin or inhaled (H302+ H312+ H332) Wear protective clothing / gloves (P280)	Firefighting measure: Suitable extinguishing media is water spray, alcohol resistant foam, dry chemical or carbon dioxide First aid measures: General advice : consult a physician If inhaled, move person to fresh air
Piperidine, acetic acid		Flammable liquids (category 2), H225 Acute toxicity, oral (category 4), H302 Acute toxicity, Dermal (category 3), H311 Skin corrosion (category 1B), H314	Fire-fighting measure : Use waterspray, alcohol-resistant foam, dry chemical or carbon dioxide First-aid measures: In case of skin contact, remove the contaminated clothes and shoes immediately.
N,N-Dimethylformamide (DMF)		Flammable liquid (category 3), H226 Acute toxicity, inhalation (category 4), H332 Acute toxicity, dermal (category 4), H312 Eye irritation (category 2), H319 Reproductive toxicity (category 1B), H360D	Fire-fighting measure: Suitable extinguishing agent is dry sand Do not use water jet First-aid measure: If inhaled, provide fresh air, In case of skin contact, wash off with soap and water
Sodium <i>tert</i> -butoxide, tri- <i>tert</i> -butyl phosphine		Flammable solids (category 1), H228 Self-heating substances and mixtures (category 1), H251 Skin corrosion (sub-category 1B), H314 Keep cool, P235	Fire-fighting measure: Use dry sand, donot use water spray First-aid measure : if swallowed, donot induce vomiting, rinse mouth with water In case of skin contact, remove contaminated clothing and shoes immediately
Palladium (II) acetate		Serious eye damage (category 1), H318	Fire-fighting measure: Suitable extinguishing media are water spray, alcohol-resistant foam, dry chemical or carbon dioxide

Toluene, hexane, ethyl acetate, acetone	   	<p>Highly flammable liquid, H225</p> <p>Aspiration hazard (category 1), H304</p> <p>Specific target organ toxicity, central nervous system, single and repeated exposures, H336 and H373</p> <p>Long-term chronic aquatic hazard, H412</p>	<p>Fire-fighting measure: suitable extinguishing media is dry sand, Do not use water jet</p> <p>First-aid measures : In case of eye contact, flush off with water</p> <p>General advice: consult a physician</p>
Chloroform- <i>d</i>	 	<p>Acute toxicity, Oral (category 4), H302</p> <p>Acute toxicity, inhalation (category 3), H331</p> <p>Skin irritation (category 2), H315</p> <p>Eye irritation (category 2), H319</p> <p>Carcinogenicity (category 2), H351</p> <p>Reproductive toxicity (category 2), H361d</p>	<p>Fire-fighting measures: Use water spray, alcohol-resistant foam, dry chemical or carbon dioxide</p> <p>First-aid measures: If inhaled, provide fresh air</p> <p>In case of eye contact, rinse thoroughly with plenty of water</p> <p>In case of skin contact, wash off with soap and water</p>
Argon		<p>Gases under pressure (compressed gas), H280</p>	<p>Fire-fighting measure: Use water spray, alcohol-resistant foam, dry chemical or carbon dioxide</p>

b) Physical factors

**Table 8.** Standard and lab reading values of physical factors

Factors	Values standards	Lithuania standards
Thermal environment	Warm period: 22.8 °C to 26.1°C Cold period : 20°C to 23.9°C [50]	HN 69:2003
Noise	$L_{ex, 8h} = 85$ dBA, $L_{cpeak} = 137$ dbc [56]	HN 33:2011
Air pollution	(8 $OU_E/m^3$ )	HN 23:2011
Illumination	1000 lumens/m <sup>2</sup> [52]	HN 98:2014

Equipment grounding	TT-system TN-system IT system	(Elektros įrenginių įrengimo taisyklės. Vilnius, 2000. 487 p [27,53] Saugos taisyklės eksploatojant elektros įrenginius, Valstybės žinios, 2001, nr. 110-4008) [27]
---------------------	-------------------------------------	--

#### c) Trauma-related physical factors

Various equipments are employed for the entire synthetic pathway of starting materials to final products. Mishandling or utilization without taking precaution of some of these could result in injuries. Few of them are listed below :

- Heating plates: hand burns
- Hot-air gun
- Glass-ware: breakage could result cuts on body

#### d) Ergonomic factors

The work involves prolonged standing, bending and repetitive hand movements in the performance of daily duties.

#### e) Psychological factors

The workload, its conditions and the interpersonal approaches within the laboratory is balanced to a an extent that it alleviates any work related stress.

### 5.3. Safe production

- Laboratory personnels should be well acquainted with all necessary safety requirements while synthesizing materials.
- Effective fume hoods with operating ventilating systems is a relevant part for performing various procedures of synthesis.
- Storage of chemicals with appropriate labels in cabinets having ventiation devices ensures safe production.
- Proper storage and disposal of used chemicals based on their properties creates safer working environment [55].

With concern to electrical safety requirements:

- The metallic parts of electrical equipments should be earthed.
- Proper insulation of electrical wirings and voltage-beaing parts should be maintained.
- The technical condition of plugs and sockets should be checked regularly.

Complying with all the above mentioned measures, the laboratory comes under the category General premises [27].

The electrical equipment neutral connection condition: All the electric equipments with 400 V and or higher alternating current and 450 V or higher voltage direct current must be grounded to prevent explosions in laboratory.

#### 5.4. Hygiene standards

**Table 9.** Working hygiene standards

Factors	Lithuanian Standard	Working standard (analyzed)
Thermal environment	HN 69:2003	Warm period: 21 °C to 28 °C Cold period: 20°C to 24 °C [50]
Noise	HN 33:2011	$L_{EX,8h} = 95$ dBA $L_{cpeak} = 130$ Dbc
Illumination	HN 98:2014	150-205 lumens/m <sup>2</sup> [52]
Equipment grounding	[53, 54]	TT-system

The limit values of occupational exposure to chemicals set by Lithuanian hygiene standards are based on long-term exposure limit (LPRD) or 8-hour reference period and short-term exposure limit (TPRD) or 15-minute reference period [51]. The occupational exposure limit of some of the chemicals used in this research work are given in the Table 10.

**Table 10.** Occupational exposure limits for chemicals [51]

Chemical substance	Threshold size						Indications of health effects
	Long-term exposure limit (LPRD)		Short-term exposure limit (TPRD)		Limit value not to be exceeded (NRD)		
	mg/m <sup>3</sup>	ppm	mg/m <sup>3</sup>	ppm	mg/m <sup>3</sup>	ppm	
Acetone	1210	500	2420	1000	-	-	-
Acetic acid	25	10	-	-	-	-	-
<i>N,N</i> -dimethylformamide	15	5	30	10	-	-	RO
Ethyl acetate	500	150	-	-	1100	300	-
Piperidine	0.2	-	-	-	-	-	O
Toluene	192	50	384	100	-	-	RO
<i>n</i> -Hexane	72	20	-	-	-	-	R

R= toxic for reproduction, O = the substance can penetrate through the body

- Personal Protective Equipment (PPE)

Based on the nature of the working environment of the laboratory and the chemical substances dealt with, the most appropriate personal protective equipment should be used. Goggles provide good eye protection as it prevents splashes of chemicals, vapours, dust and mist from going into eyes. Vinyl and neoprene gloves could be preferred as it shields hands against toxic chemicals. In addition to

these, for foot protection various safety shoes and boots like butyl or vinyl or nitrile footwear could be selected. The right kind of body protection could be aprons and sleeves but while handling certain hazardous substances chemical resistant full body suit would be apt.

### **5.5. Fire safety**

On the basis of characteristics of the materials used and the technological processes employed, suitable fire-fighting and neutralizing steps should be adopted. All equipments especially electrical should not be left unattended. The laboratory space should be properly ventilated before and after completing work [55]. If a fire occurs, a student must inform fire prevention service immediately using the emergency number ,112‘ as well as the laboratory work supervisor. Carbon-dioxide extinguishers are used for all operating electrical equipments [27].

## Conclusions

Intermediate and final four coumarin-based compounds were designed and synthesized by Knoevenagel condensation and Buchwald-Hartwig reactions.

1. The coumarin derivatives demonstrated high thermal stability with 5% weight loss temperatures in the range from 310 to 356 °C. Glass forming abilities were observed for all the coumarin derivatives, of which considerably higher glass transition temperature was found in *para* substituted coumarin derivative, (**NS-8a**, 120 °C).
2. Strong intramolecular charge transfer was noted as a result of the combination of coumarin substituted with fluorocarbons at different positions as core acceptor moieties and strong donor phenoxazine and was confirmed by solvatochromism in emission spectra.
3. The ionization potential values estimated by cyclic voltammetry were same (5.09 eV) and electron affinity were in the range from 1.74 eV to 1.69 eV.
4. All the structures were optimized and theoretical values of HOMO and LUMO were calculated.
5. The dilute solutions as well as the films of the coumarin derived compounds exhibited fluorescence ranging from 612-677 nm and 605-665 nm. Large Stokes shifts were observed for all compounds except coumarin derivative **NS-5a**. The solid films of the coumarin derivatives showed fluorescence quantum yields in the range from 0.3 to 0.8.
6. The characteristics ( good thermal stability, reasonable electrochemical stability and fluorescence quantum yields) of the coumarin derivatives might make them promising electroluminescent materials for optoelectronic applications. A technological line for the production of the derived compounds was designed and proposed.

## Acknowledgements

Principally, I would like to thank *Almighty God* for His constant grace and presence, only by which this endeavour came into being.

I would like to acknowledge *Kaunas University of Technology and Faculty of Chemical Engineering*, for all the facilities and services provided during the course of my study. My special thanks to *Prof. Juozas Vidas Grazulevicius* for giving me this opportunity to conduct my thesis in his research group. I am deeply grateful to my supervisor *Dr. Dalius Gudeika* for his invaluable guidance and support throughout the period of my work. I am enormously indebted to him for patiently teaching me all the requisites, techniques mechanisms and procedures of organic synthesis. I am also thankful to *Lect. Gintare Krucaite* for reviewing my Master Thesis.

I would like to express my gratitude to all my colleagues in the lab as well as the entire research group for their input and friendship. My sincere thanks to PhD students *Naveen Masimukku* and *Ronit Sebastine Bernard* and lab. colleagues, *Simas Macionis* and *Kestutis Dabrovolskas* for their continuous help in various parts of my research work. I am grateful to all professors, students and other researchers who contributed to the completion of this work. I specially thank *Dr. Joana Bendoraitiene* and *Dr. Ramune Rutkaite* for providing me a chance to undertake research in the laboratory I worked.

Finally, my heartfelt thanks to my parents and siblings for their love and support that helped me throughout my life. Words would never be enough for their sacrifices rendered for making me to the person I am today.



## List of publications

- Samuel, Nizy Sara; Gudeika, Dalius. Design, synthesis and investigation of coumarine-based derivatives // Open Readings 2020: 63<sup>rd</sup> international conference for students of physics and natural sciences, March 17-20, Vilnius, Lithuania. Vilnius: Vilnius University. 2020, p. 1.

## List of references

1. ADACHI, C., Third-generation organic electroluminescence materials. *Japanese Journal of Applied Physics*. 2014, 53(6), pp 060101. ISSN 0021-4922
2. RANA, R. et al., An extensive review on organic light-emitting diode for energy-saving and eco-friendly technology. In: Mishra S., Sood Y., Tomar A. eds. *applications of computing, automation and wireless systems in electrical engineering: MARC Proceedings*. Springer Singapore. 2019, pp 891-912. ISBN: 978-981-13-6772-4
3. KERUKIENE, R., Synthesis and properties of indole-based electroactive compounds, *Daktaro Disertacija*. Kaunas: Kauno technologijos universitetas. Prieiga per eLABa – nacionalinę Lietuvos akademinę elektroninę biblioteką, 2017
4. YANG, X., et al., Recent advances of the emitters for high performance deep-blue organic light-emitting diodes. *Journal of Materials Chemistry C*. 2015, 3(5), pp 913-944. ISSN 2050-7526
5. PHADTARE, S.B., et al., Greener Protocol for one pot synthesis of coumarin styryl dyes. *Dyes and Pigments*. 2013, 97(1), pp 105-112. ISSN 0143-7208
6. CHRISTIE, R.M. and LUI, C.H., Studies of fluorescent dyes part:2. An investigation of the synthesis and electronic spectral properties of substituted 3-(2'-benzimidazolyl) coumarins, *Dyes and Pigments*. 2000, 47(1), pp 79-89. ISSN 0143-7208
7. MEI, L., et al., The inductive effect of electron-withdrawing trifluoromethyl for thermally activated delayed fluorescence: tunable emission from tetra to penta-carbazole in solution processed blue OLEDs, *Chemical Communications*. 2015, 51(65), pp 13024-13027. ISSN 1359-7345
8. TANAKA, H., et al., Efficient green thermally activated delayed fluorescence (TADF) from a phenoxazine-tri-phenyl triazine (PXZ-TRZ) derivative, *Chemical Communications*. 2012, 48(93), pp 11392-11394. ISSN 1364-548X
9. ZENG, W., et al., Achieving nearly 30% external quantum efficiency for orange-red organic light-emitting diodes by employing thermally activated delayed fluorescence emitters composed of 1,8-Naphthalimide-Acridine hybrids, *Advanced Materials*. 2018, 30(5), pp 1704961. ISSN 0935-9648
10. BELLIS, M., *OLED: Technology guidelines and History*. DotDash, ed. Olivia Valdes [online]. 2019 [viewed 11 02 2020]. Available from: <https://www.thoughtco.com/who-invented-oled-technology-1992208>
11. KARZAZI, Y., *Organic light emitting diodes: Devices and applications*, *Journal of Materials and Environmental Science*. 2014, 5(1), pp 1-12. ISSN: 2028-2508, Available from: <http://www.jmaterenvironsci.com>
12. FICHOU, D. and HOROWITZ, G., *Molecular and polymer semiconductors, conductors and superconductors: Overview*. Buschow et al ed., Oxford: Elsevier, 2001. ISSN 9780-080431529. Available from: <https://doi.org/10.1016/B0-08-043152-6/01000-7>
13. TREMBLAY, J.F., The rise of OLED displays. *C&EN Global Enterp*, 2016, 94, no. 28. pp 30-34. ISSN 0009-2347. Available from: <https://doi.org/10.1021/cen-09428-cover>
14. LU, S.Y., et al., Virtual screening of hole transport, electron transport, and host layers for effective OLED design. *Journal of Chemical Information and Modelling*. 2018, 58(12), pp 2440-2449. ISSN 1549-9596

15. GODUMALA, M., et al., Recent breakthroughs in thermally activated delayed fluorescence organic light emitting diodes containing non-doped emitting layers. *Journal of Materials Chemistry C*, 2019, 7(8), pp 2172-2198. ISSN 2050-7526
16. LU, J., et al., Rational design of phenoxazine-based donor-acceptor-donor thermally activated delayed fluorescent molecules with high performance. *Physical Chemistry Chemical Physics*, 2015, 17(30), pp 20014-20020. E-ISSN: 1463-9084
17. TADF: What is thermally activated delayed fluorescence?, In: Research and publications. Edinburgh Instruments blog, [viewed on 10 03 2020]. Available from: <https://www.edinst.com/blog/tadf-thermally-activated-delayed-fluorescence>
18. BIZZARRI, C., et al., Triplet emitters versus TADF emitters in OLEDs : A comparative study. *Polyhedron* , 2018, 140, pp 51-66. ISSN 0277-5387
19. VOLZ, D., Review of organic light-emitting diodes with thermally activated delayed fluorescence emitters for energy-efficient sustainable light sources and displays. *Journal of Photonics for Energy*, 2016, 6(2), pp 020901-020901. E-ISSN: 1947-7988
20. ALHAMA, A.E. et al., TADF technology for efficient blue OLEDs :Status and challenges from an industrial point of view, In:Luminescence: OLED Technology and applications[working title], ed.Pyshkin S.L. [online]. InTech, 2019 [viewed 20 01 2020]. Available from: <https://www.intechopen.com/online-first/tadf-technology-for-efficient-blue-oleds-status-and-challenges-from-an-industrial-point-of-view>
21. TORGOVA, S. and STRIGAZZI, A., Organic electroluminescent materials. *Molecular Crystals and Liquid Crystals*, 2002, 375(1), pp 61-72. E-ISSN: 1563-5287
22. SHIROTA, Y. and KAGEYAMA, H., 1-Small molecular weight materials for (opto)electronic applications:Overview. In *Handbook of organic materials for optical and (opto)electronic devices* pp 3-82. Elsevier. 2013. ISBN 9780-857092656
23. WEI, Q., et al., Small molecule emitters with high quantum efficiency :mechanisms, structures and applications. *Advanced Optical Materials*. 2018, 6(20), pp 1800512, ISSN 2195-1071
24. CHEN, J., et al., Highly efficient thermally activated delayed fluorescence emitters based on novel Indolo[2,3-b]acridine electron-donor. *Organic Electronics*. 2018, 57, pp 327-334, ISSN 1566-1199
25. PASHAZADEH, R., et al., An iminodibenzyl-quinoxaline-iminodibenzyl scaffold as a mechanochromic and dual emitter donor and bridge effects on optical properties, *Chemical Communications*. 2018, 54(98), pp 13857-13860. ISSN 1359-7345
26. YANG, Z., et al., Recent Advances in organic thermally activated delayed fluorescence materials. *Chemical Society Reviews*, 2017, 46(3), pp 915-1016. ISSN 0306-0012
27. BERNARD, R.S., Synthesis and properties of triphenylethylene derivatives containing carbazole and acridine moieties. *Magistro darbas, Kauno technologijos universitetas*.2018, pp 70
28. GENSICKA-KOWALEWSKA, M., et al., Recent developments in the synthesis and biological activity of acridine/acridone analogues. *RSC Advances*, 2017, 7(26), pp 15776-15804. ISSN: 2046-2069
29. KUMAR, A., et al., Substitution effects on the optoelectronic properties of coumarin derivatives, *Applied Science*. 2020, 10(1). ISSN 2076-3417
30. RAO, H.S., et al., Photophysical behaviour of a new cholestrol attached coumarin derivative and fluorescence spectroscopic studies on its interaction with bile salt systems and lipid bilayer membranes, *Physical Chemistry Chemical Physics*, 2014, 16(3), pp 1247-1256. ISSN 1463-9076

31. MATTA, A., et al., Synthesis, characterisation and photophysical studies of oxadiazolyl coumarin: A new class of blue light emitting fluorescent dyes. *Dyes and Pigments*. 2017, 140, pp 250-260, ISSN 0143-7208
32. TASIOR, M., et al.,  $\pi$ -expanded coumarins: Synthesis, optical properties and applications, *Journal of Material Chemistry C*, 2015, 3(7), pp 1421-1446. ISSN 2050-7526
33. KIM, T. and SWAGER, T.M., A Fluorescent self-amplifying wavelength -responsive sensory polymer for fluoride ions. *Angewandte Chemie International Edition*, 2003, 42(39), pp 4803-4806. ISSN 1433-7851
34. LONCARIC, M., et al., Recent advances in the synthesis of coumarin derivatives from different starting materials. *Biomolecules*, 2020, 10(1). ISSN 2218-273X
35. CHEN, J., et al., Coumarin-based thermally activated delayed fluorescence emitters with high external quantum efficiency and low efficiency roll-off in the devices. *ACS Applied Materials and Interfaces*, 2017, 9(10), pp 8848-8854. ISSN 1944-8244
36. LI, Y., et al., Polycyclic aromatic hydrocarbon-bridged coumarin derivatives for organic light-emitting devices. *Arabian Journal of chemistry*, 2020, 13(2), pp 4126-4133. ISSN 1878-5352
37. WANG, B., Realizing efficient red thermally activated delayed fluorescence organic light-emitting diodes using phenoxazine/phenothiazine-phenanthrene hybrids. *Organic Electronics*, 2018, 59, pp 32-38. ISSN 1566-1199
38. HAN, L., et al., Synthesis and density functional theory study of novel coumarin-type dyes for dye sensitized solar cells, *Journal of Photochemistry and Photobiology A : Chemistry*, 2014, 290, pp 54-62. ISSN 1010-6030
39. KATO, Y., et al., A sky blue thermally activated delayed fluorescent emitter to achieve efficient white light emission through in situ metal complex formation. *Journal of Material Chemistry C.*, 2019, 7(11), pp 3146-3149. ISSN 2050-7526
40. XU, R., et al., *Introduction to natural products chemistry*. CRC Press, 2011. ISBN 9781439860779
41. Jigar, L.P., *The introduction of coumarin*, BlueRose Publishers, 2019, 1, pp 432. ISBN 978-93-5347-587-1
42. ZHANG, Y., Suppressing efficiency roll-off of TADF based OLEDs by constructing emitting layer with dual delayed fluorescence, *Frontiers in Chemistry*. 2019, 7, pp 302. E-ISSN: 2296-2646
43. MATULAITIS, T., *Studies of synthesis and properties of bipolar compounds for organic optoelectronic devices : Doktoro Disertacija*. Kaunas: Kauno technologijos universitetas. Prieiga per eLABa – nacionaline Lietuvos akademine elektronine biblioteka, 2018.
44. LUO, Q., et al., Synthesis and characterization of 9, 10-[di-P-(7-diethylamino-coumarin-3-yl) thiophenyl] anthracene as fluorescent material. *Journal of sulfur chemistry*, 2018, 39(1), pp. 89-98. ISSN 1741-5993
45. SCILLA, C.T., *Systematic synthesis of organic semiconductors with variable bandgaps*, 2012, *Open Access Dissertations*, 603. [https://scholarworks.umass.edu/open\\_access\\_dissertations/603](https://scholarworks.umass.edu/open_access_dissertations/603)
46. PLUCZYK, S., et al., Using cyclic voltammetry, UV-Vis NIR and EPR spectroelectrochemistry to analyze organic compounds. *Journal of Visualized Experiments*. 2018, 140. E-ISSN: 1940-087X

47. BUCKLEY, A., Organic light-emitting diodes (OLEDs): Materials, devices and applications, Woodhead Publishing series in electronic and optical materials, 2013, 36. ISBN 978-0-85709-894-8 (online)
48. Acros-Ramos, R., et. al., 3-substituted-7-(diethylamino) coumarins as molecular scaffolds for bottom-up self-assembly of solids with extensive  $\pi$ -stacking. Journal of Molecular structure, 2017, 1130, pp 914-921. ISSN 0022-2860
49. Safety data sheet of all compounds and statements [online]. In Sigma Aldrich, 2020 [viewed on 20 04 2020], Available from: <http://sigmaaldrich.com/european-export.html>.
50. HN 69:2003. Šiluminis komfortas ir pakankama šiluminė aplinka darbo patalpose. Parametru norminės vertės ir matavimo reikalavimai. Valstybės žinios, 2004, Nr. 45-1485
51. HN 23:2011. Cheminių medžiagų profesinio poveikio ribiniai dydžiai. Matavimo ir poveikio vertinimo bendrieji reikalavimai. Valstybės žinios, 2011, Nr. 112-5274
52. HN 98:2014. Natūralus ir dirbtinis darbo vietų apšvietimas. Apšvietos ribinės vertės ir bendrieji matavimo reikalavimai. TAR, 2014, Nr. 05119
53. Elektros įrenginių įrengimo taisyklės. Vilnius, 2000. 487 p
54. Dėl Specialiųjų patalpų ir technologinių procesų elektros įrenginių įrengimo taisyklių patvirtinimo. Valstybės žinios, 2013, Nr. 27-1299
55. Bendrosios gaisrinės saugos taisyklės. Valstybės žinios, 2010, Nr. 99 -5167 (Aktuali redakcija: Valstybės žinios Nr. 118-5970).
56. HN 33:2011. „Triukšmo ribiniai dydžiai gyvenamuosiuose ir visuomeninės paskirties pastatuose bei jų aplinkoje“. Valstybės žinios, 2011, Nr. 75-3638